

# 1

---

## Mechanics in Tumor Growth

L. GRAZIANO

*Polytechnic of Turin  
Department of Mathematics  
I-10127 Torino, Italy*

AND

L. PREZIOSI

*Polytechnic of Turin  
Department of Mathematics  
I-10127 Torino, Italy*

**ABSTRACT.** This chapter focuses on the mechanical aspects of tumor growth. After describing some of the main features of tumor growth and in particular the phenomena involving stress and deformation, the chapter deals with the multiphase framework recently developed to describe tumor growth and shows how the concept of evolving natural configurations can be applied to the specific problem. Some examples are then described according to the type of constitutive equation used, specifically focusing on contact inhibition of growth, nutrient limited avascular growth and interaction with the environment.

---

## 1 Introduction

The attempt to give a unified description of what a tumor is, unfortunately is still hopeless, both because there are several tumors with different origin and characteristics and because there are several concurrent causes of tumor development. Using probably a naive description, one can say that the cells forming a compact tumor, like other cells in the body, live in a watery environment full of proteins. These include all sorts of nutrients the cell need to survive and duplicate, and chemical factors, in particular growth promoting factors, growth inhibitory factors, and chemotactic factor, which trigger sub-cellular chemical pathways determining the behavior of the cell. The extracellular space is also filled of a network of cross-linked proteins (e.g., elastin, collagen, proteoglycans) collectively known as extracellular matrix (ECM), which form the structure of the tissue.

Both in a physiological situation and in a pathological one, the interactions that a cell has with its neighbors and with the extracellular matrix is very complex. In particular, focusing on the physiological behavior, cells pull on the extracellular matrix to move and want to be attached to it to duplicate. They like the growth factors and proteins embedded in the extracellular matrix and continuously remodel it by digesting part of the ECM or cleaving some of the constituents by the continuous production of matrix degrading enzymes, e.g., matrix metallo-proteinases (MMP). At the same time, some cells (in particular fibroblasts) rebuild the extracellular matrix. As will be described in the following this process is affected by the stress applied to the tissue, as it can be easily understood by recalling bad experiences (hopefully not personal) like the therapeutic action of braces and the traction applied to heal a fractured bone, or just the fact that exercise and physical training have a good effect on our body while prolonged rest are detrimental for both bones and muscles.

Cells also prefer to feel the presence of other cells of the same type, either by the transduction of specific chemical signals or by cell contact. If they feel lonely they commit suicide by a process called anoikis.

On the other hand, a cell replicates if it senses that there is sufficient space for doing it or if they are chemically stimulated. Conversely, if they sense that there is a sufficient number of cells around, they can alter their activity and enter a quiescent state ready to re-activate their replication programme if, for instance, a neighboring cell dies.

Most of the complex processes briefly sketched above are influenced by the production and reception of chemical signals. In most cases the behavior of a cell depends on the balance between two (or more) contraddictory signals. For instance, mitosis can be stimulated by the overexpression of a

growth promoting signal or by the underexpression of a growth inhibitory signal. An excessive presence of extracellular matrix can be caused by the excessive production of ECM, by a decreased production of matrix degrading enzymes (MDEs), or by an increased production of tissue inhibitors of metallo-proteinases (TIMPs), that is, the molecules that make MDEs ineffective, so that even if the production of MDEs is normal their effect is damped by TIMP upregulation.

The behavior of a cell also depends on the balance between chemical and mechanical inputs, so that a cell might give up duplication for the presence of growth inhibitory factors in spite of the fact that there is space around, or viceversa might duplicate stimulated by growth promoting factors, in spite of the lack of space.

This is not a pathological situation. For instance, in wound healing the endothelial cells covering the wall of a capillary duplicate in response to the stimulus of vascular endothelial growth factors (VEGF) produced by hypoxic cells in spite of the absence of any mechanical stimulus. Cells then move toward the injury forming new capillaries to bring the materials necessary for healing the cut.

In this scenario, how can then a normal tissue generate a hyperplasia and then a tumor? The reasons can be disparate but, generally speaking, have to do with the occurrence of some failure in the complex mechanisms controlling the “circle of life”, including the following:

- the cell becomes insensitive to growth inhibitory signals, for instance losing retinoblastoma suppressor;
- the cell produces growth promoting signals, for instance activating H-Ras oncogene;
- the cell delays apoptosis, i.e., natural death, for instance producing IGF survival factors;
- the cell completely loses its program-to-death, becoming immortal;
- the cell acquires a limitless replicative potential by turning on telomerase;
- the cell becomes insensitive to mechanical cues, the so-called cadherin switch;
- the cell does not need to be properly attached to the ECM, the so-called integrin switch;
- the cell does not need to feel the presence of similar cells to survive;

where the last two characteristics are linked to the diffusion of metastasis and the formation of secondary tumors.

The problem is then very complex. The majority of the models present in the literature focus on the chemical aspects of tumor growth, which is however fundamental, and are based on reaction-diffusion equations and mass balance equations with suitable closure for the velocity field. For a more detailed discussion on these aspects, the interested reader is referred to the books [1, 29, 79] and the special issues [12, 27, 28] specifically devoted to tumor modelling, and to the recent review articles [6, 66] where even more references can be found. In fact, in this chapter we will only focus on the mechanical aspects of tumor growth, which include the effect of stress on cell growth and apoptosis, the involvement of stress on the surrounding tissue, or simply the link between stress and deformation in deducing tumor growth models. Therefore, the effect of chemical factors will play here a secondary role, though we are well aware of their importance. Actually, even when focusing on the mechanical aspects of tumor growth, it is clear that the duplication or death of cells is chemically regulated inside the cell. So, at some stage, the mechanical signal has to be translated into a chemical message that goes to the nucleus and determines the behavior of the cell.

The main advantage of the introduction of such a mechanical framework is in the ability to deal with stress, with its influence on the evolution of the tissue itself, and with the mechanical interaction with other surrounding tissues. The main limitation is due to the fact that data on the response of multicell aggregates to traction and compression are not available yet for tumors, though similar studies have been done for other tissues (mainly bones and cartilages, but also brain, lungs, heart, skin, and so on). Furthermore, in order to use models with many constituents it is necessary to discriminate the stress contribution due to the different constituents. However, in our opinion, once the experiments are done the modelling framework has a great potential.

---

## 2 Mechanics and Mechanotransduction in Tumor Growth

### 2.1 Cadherin Switch

In a normal tissue the rate of proliferation decreases when cells come in contact, a phenomenon often called contact inhibition of growth [36, 37, 56, 72, 78, 85]. A quantification of this phenomenon is represented in Fig. 1 that reports some experimental results by Tsukatani et al. [92] on human

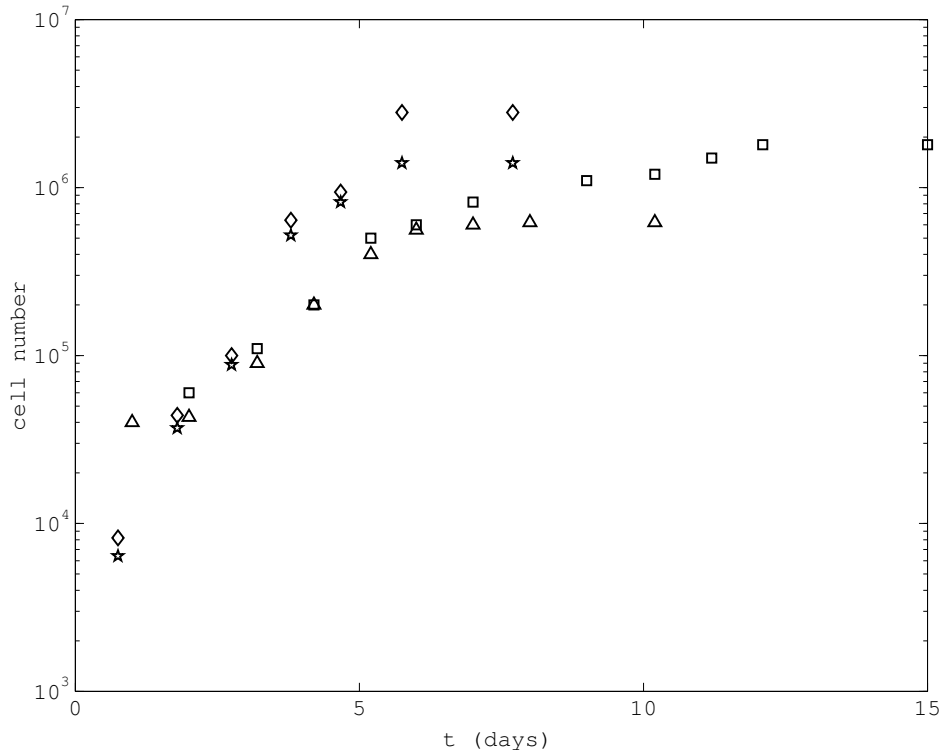


Figure 1: Examples of contact inhibition of growth reported in the experiments by Tsukatani et al. [92] using human breast epithelial cells (Squares = late passage and triangles = early passage) and by Orford et al. [74] using canine kidney-derived nontransformed epithelial cells (stars = wild type and diamonds = S37A mutant).

breast epithelial cells grown in vitro over a suitable substratum and by Orford et al. [74] on canine kidney-derived nontransformed epithelial cells.

It can be seen that after an initial exponential growth cell density saturates forming a monolayer of cells. On the other hand, “tumor” cells continue proliferating forming a multilayer leading to the conjecture that they need to feel more contacts or a larger pressure to stop their proliferation program.

The starters of this growth control mechanism are the cadherins, the transmembrane receptors involved in homophilic cell-cell interactions, because of their crucial role in cell-cell adhesion and in mechanotransduction [62, 72, 85, 87, 89, 92, 95] (see Fig. 2).

Their involvement has been checked in several ways. For instance, Warhol [96] spread synthetic beads coated with N-cadherin ligands over a

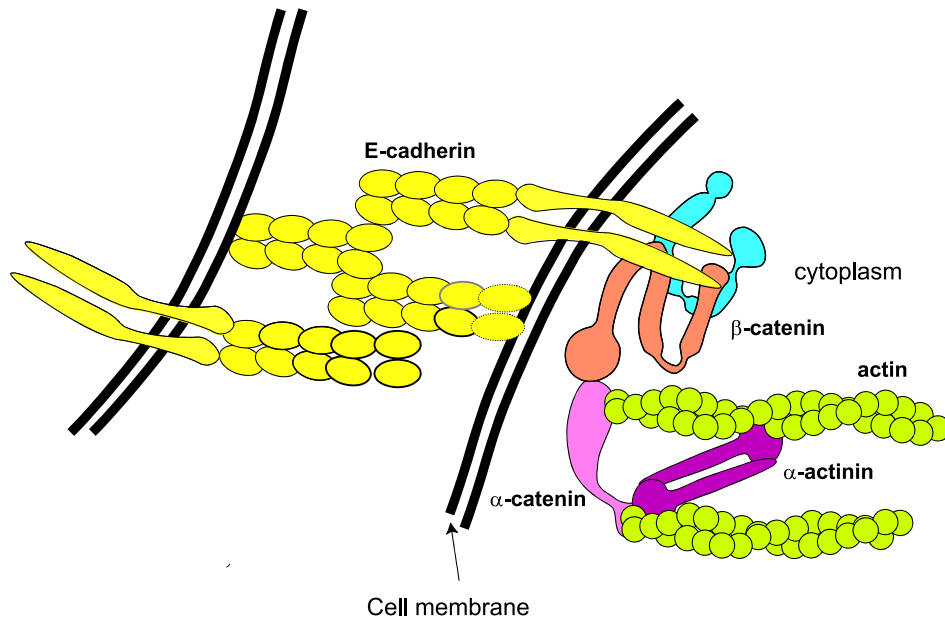


Figure 2: Cadherin-cadherin junction.

substratum and seeded some cells on it. They then found that due to the interaction with the beads cells stopped duplicating. Similarly, Caveda et al. [25] found that coating the underlying substratum with the extracellular domain of recombinant VE-cadherin suppressed cell proliferation. Conversely, Castilla et al. [23] found that the disruption of the intercellular cadherin junctions triggers the production of growth factors which contribute to induce proliferation.

On the basis of these observation, it is clear that if a cell is not so sensitive to the control mechanisms above it is subject to deregulated growth, a phenomenon that is considered such an important milestone in the development of tumors to deserve to be named “cadherin switch” in analogy with the “angiogenic switch” leading to the vascularization of tumors which will be briefly described in Section 2.4.

In fact, it is known that loss of contact responsiveness is commonly associated with the formation of hyperplasia and malignant transformation such as gastric carcinoma [11, 73], adenocarcinoma [93], epithelial tumors [24, 32], colon polyps and carcinoma [48], gynecological cancers [83], intimal thickening [94] (see also the review by Hajra and Fearon [49]).

However, cadherins only represent the tip of the iceberg. They are more visible than other hidden players for their transmembrane location, but there are many other candidates that can be responsible of a possible

incorrect mechano-transduction. The second family of suspects are the catenins, the proteins cadherin link to for a functional cell-to-cell adhesion (see Fig. 2). In fact, Stockinger et al. [87] showed that epithelial cells exhibited a strong  $\beta$ -catenin activity at low densities ( $\leq 40\%$  confluency), which was five- to seven-fold reduced when cells reached a confluency  $> 80\%$ . In fact, it is thought that in physiological conditions upon reaching confluency the expressed cadherins sequester catenins downregulating their activity. Since it is known that the upregulation of catenins is necessary for cell duplication, as we shall see in the following and is sketched in Fig. 3, the final result is that cell adhesion negatively affects cell proliferation.

To test the link between cadherins and catenins Caveda et al. [31] transfected Chinese Hamster Ovary cells with a cytoplasmic truncated mutant of VE-cadherin. They found that the deletion of the cytoplasmic tail of VE-cadherin abolishes its growth inhibitory activity without affecting its adhesive properties.

More in detail, Dietrick et al. [37] explain the mechanism of contact inhibition of growth as follows:

- tissue compression and overexpression of cadherins cause the under-expression of catenins,
- the underexpression of catenins determines the accumulation of the cyclin-dependent kinase (cdk) inhibitors p16, p21, and p27,
- their overexpression inhibits the entry in the S phase causing cell cycle arrest in the G1 phase [33, 56, 78]. More in detail, referring to Fig. 3,
  - p16 blocks the activity of cdk4 by dissociating cyclin D from cdk4 and binding to cdk4,
  - p27 inhibits cdk2-cyclin E activity directly by binding to the complex.

In Fig. 3, the process above is schematized by reading the bold words as underexpressed proteins. Conversely, reading them as overexpressed quantities one has for instance that upregulation of catenins leads to the expression of cyclin dependent kinase and then to DNA replication and mitosis. This procedure is particularly useful for linear cascades, while it may fail in the presence of feedback loops.

In order to fully exploit the protein cascade in tumor modelling, one should have all the affinity constants and reaction rates, which at present is not the case. In addition, the spatial localization of the proteins involved in the cascade should be also taken into account. So, at present, the way generally used in the literature is to proceed, whenever possible, with a

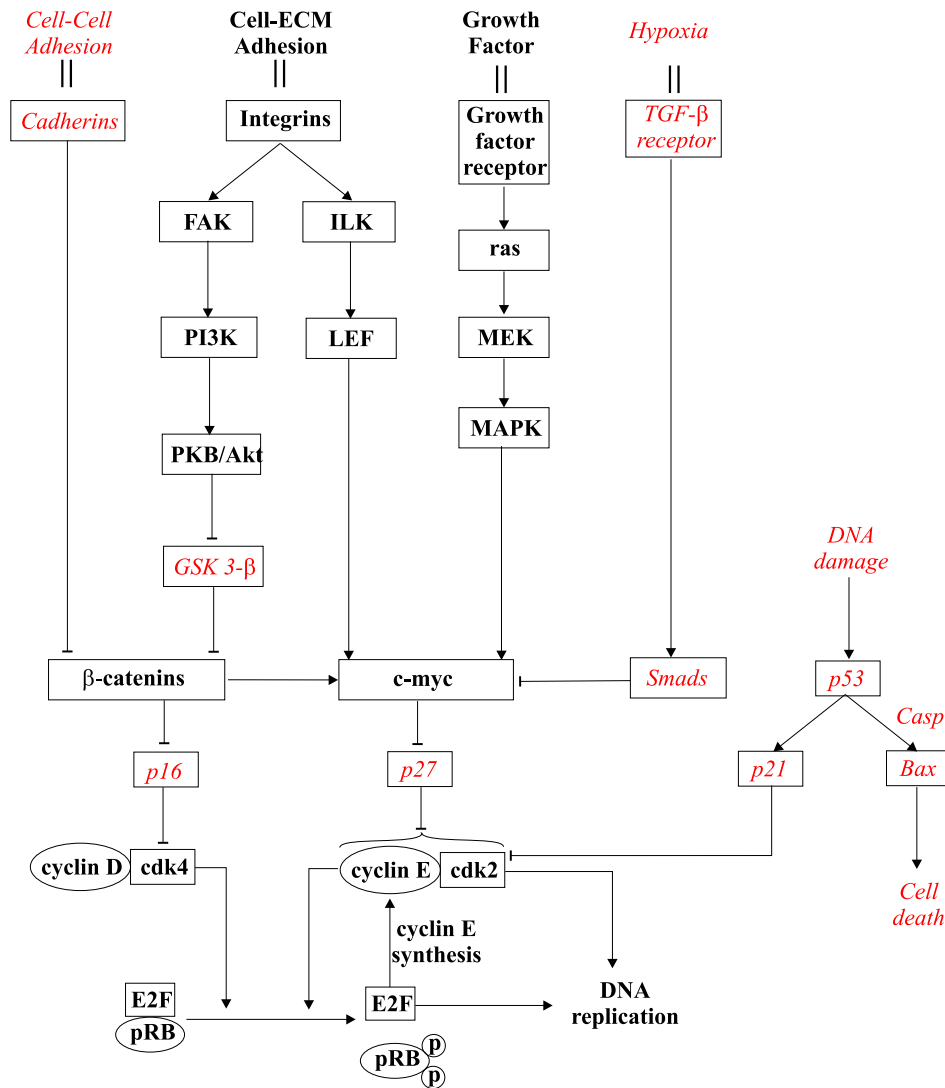


Figure 3: Sketch of some protein cascades involved in the cell-cycle and in particular of those involving cadherins, integrins and catenins. In order to put in evidence the on-off mechanisms, arrows, corresponding to stimulatory activities, connect proteins with the same fonts, while blockades, corresponding to inhibitory activities, connect proteins written using different fonts. At the end, forgetting the details of the cascades, one can for instance extract that cell-cell adhesion inhibits proliferation. cdk stands for cyclin-dependent kinase, pRB for hypophosphorilated retinoblastoma, and the added p's indicate its phosphorylation. The curly bracket indicates that p27 binds to the cdk2/cyclin complex.

Tissue [source]	Water	Collagen	Proteo- glycans	Elastin
Intervertebral disk Nucleus pulposus Annulus fibrosus [41]	80%	5%	13%	
Aorta [70]	65%	9%	1%	16%
Articular cartilage (femoral) [70]	80%	13%	5%	trace
Corneal stroma [69, 91]	77%	16%	1%	
Ligament (cruciate) [98]	68%	25%	1%	<1.6%
Meniscus [?]	74%	23%	1%	trace
Skeletal muscle [63]		14%		
Tendon [58, 98]	55-70%	25%	0.5%	<1%
Skin [98]	60%	26%	1%	2-4%
Subcutaneous tissue [63]		21%		
Prostate cancer [100]		7%-26%		

Table 1: Constituents of several tissues. Notice the strong variability in the collagen content of prostate cancer which depends on the grade of the tumor.

spatially homogeneous Boolean reasoning, which means using on/off relationships. For this reason in Fig. 3 we tried to highlight the overexpressed and underexpressed proteins by using different fonts.

## 2.2 Interaction with the Extracellular Matrix and Integrin Switch

Another main component of both normal and tumor tissues is the extracellular matrix (ECM), a fibrous structure which is composed by many constituents produced by a variety of stromal cells, mainly fibroblasts. The ECM is constantly renewed through the concomitant production of matrix metalloproteinases (MMP) and new ECM components.

In stationary conditions the remodelling of ECM is a slow process. For instance, in the human lung the physiological turnover of ECM is 10-15% per day [54], which leads to an estimated complete turnover in a period of nearly a week. However, when a new tissue has to be formed, e.g. to repair a wound, then the rate of production is one or two order of magnitude faster [31, 35]. Hence, it seems that also the production of ECM constituents is affected by the pressure felt by the cells. However, this relation is rather complicated. It is, for instance, well known that for bones, teeth, and muscles [57, 58, 67] the remodelling process is strongly affected by the stresses and strains the tissue is subject to. This is a physiologically

Tissue	Elastic modulus (Pa)
Normal mammary gland	$167 \pm 31$
Average breast tumor	$4049 \pm 938$
Stroma attached to tumor	$916 \pm 269$
Reconstituted basement membrane	$175 \pm 37$
Collagen (2.0 mg/ml)	$328 \pm 87$
Collagen (4.0 mg/ml)	$1589 \pm 380$

Table 2: Examples of elastic moduli of normal and abnormal breast tissue and stroma (data from [77]).

functional process because it allows to keep the stroma young and reactive. In fact, prolonged rest or space flight are detrimental for bones and muscles, while exercise and physical training have an opposite effect.

The percentage of ECM content changes considerably from tissue to tissue (see Table 1) from normal to tumor tissues, and also within the same tumor with tumor progression (see [100]). For instance, Takeuchi et al. [90] found that breast tumors presented a denser and more fibrous stroma with several differences in the chemical composition. On the other hand, it is well known to everybody that the first hints on the possible presence of a breast nodules are obtained by palpating the breast and feeling stiffer regions (see Table 2). Increased presence of ECM was also observed in other pathologies like cardiac hypertrophy, intima hyperplasia, cardiac fibrosis, liver fibrosis, pulmonary fibrosis, asthma, glomerulonephritis, colon cancer [16, 54, 65, 81].

The alteration in the ECM composition can be due to several probably concurring reasons:

- increased synthesis of ECM proteins;
- decreased activity of matrix degrading enzymes (MDEs);
- upregulation of tissue-specific inhibitors of metalloproteinases (TIMPs).

On the other hand, excessive degradation of ECM due to excessive production of MMP-13 characterizes chronic inflammatory diseases such as osteoarthritic cartilage, rheumatoid synovium, chronic ulcer, intestinal ulcerations, periodontitis, and many malignant tumors [99].

The interaction between ECM and cells is very important because cells need to properly adhere in order to survive. They only duplicate if they are anchored to the ECM. As shown in Fig. 3, the mechano-transduction cascade is mainly activated by integrins.

On the other hand, in the process of invasion and formation of metastases tumor cells detach from the original site, invade the surrounding tissue, intravasate entering the blood or lymphatic system, and extravasate to reach a secondary site. It is then clear that the formation and diffusion of metastases require that cells acquire the ability of surviving without interacting with the ECM. In fact, like for cadherins, it is found that tumors have altered integrins. This, in turn, alters the downstream integrin signalling pathway, so that one could argue that there is an integrin switch in addition to the mentioned cadherin and angiogenic switches.

Actually, Paszek et al. [77] prove that through the integrin signalling pathway the stiffness of the ECM promote malignant behavior consisting in growth enhancement and loss of tissue polarity which for instance leads to the absence of lumen formation in ductal carcinoma and the formation of hyperplasia, the first step toward tumorigenesis.

### 2.3 Nutrient Limited Growth and Tumor Structure

In order to give a more complete picture of the dynamics of tumor growth we need to mention some important effects which are related to the contribution of nutrients and vascularization in tumor growth. In particular, the former has to do with the existence of a nutrient limited dimension of the tumor. We will not enter in details because nutrient limited growth has little to do with mechanics, which is the focus of this chapter and refer to [6] for a recent descriptive and detailed review.

Generally speaking, tissues receive vital nutrients and oxygen perfusing through the vessel wall and diffusing in the extracellular space. When tumor cells cluster in a tissue forming a multicellular spheroid they receive their nutrients through the boundary of the tumor. Nutrients then diffuse toward the center of the tumor. When the tumor is small, all cells are well-nourished and proliferate rapidly. As the colony increases in size, due to the strong metabolic activity characterizing tumor cells, the cells towards the center are progressively starved of oxygen and nutrients and, as a consequence, their proliferation rate decreases. If the oxygen concentration falls below a critical threshold value then the cells are unable to survive and undergo cell death generating a necrotic core.

Eventually avascular tumors will reach an equilibrium size ( $\sim 2$  mm in diameter [43]), at which the rates of cell proliferation and apoptosis, averaged over the tumor volume, balance. At this stage the tumor typically comprises an outer rim of proliferating cells, a central core of necrotic debris and an intermediate region of quiescent cells which are alive, but do not proliferate due to nutrient deprivation [88].

## 2.4 Angiogenic Switch

The switch from the slow and relatively harmless avascular growth phase described above to the rapid and life-threatening vascular growth phase occurs during a process termed angiogenesis [22, 34, 42]. We will briefly describe them in the following, though the interested reader can find more information on the process in the recent reviews by Bussolino et al. [18] and by Mantzaris et al. [66].

It is possible to divide the angiogenic process into the following well differentiated stages which sometimes partially overlap:

1. Due to the lack of oxygen and nutrients certain tumor cells secrete a range of diffusible proteins and chemicals that are known collectively as tumor angiogenic factors (TAFs), in particular vascular endothelial growth factors (VEGF).
2. The reception of TAFs causes a loss of interconnection between the endothelial cells that line the blood vessels, and a reduction of vascular tonus. This in particular induces an increase in the vessel permeability.
3. TAFs also stimulate the endothelial cells to release some proteolytic enzymes (serine-proteins, iron-proteins) which degrade the basement membrane surrounding the capillary facilitating cell movement, to proliferate, and to migrate chemotactically, i.e. up the TAF gradient, towards the source of angiogenic stimulus, that is the tumor.
4. Capillary sprouts then form by the accumulation of endothelial cells. The stage of differentiation is characterized by the exit of the endothelial cells from the cell cycle and by their capacity of surviving in sub-optimal conditions and of building themselves primitive capillary structures, not yet physiologically active.
5. When capillary tips come into close proximity, they fuse together by a process called anastomosis, forming closed loops through which blood may circulate. Secondary sprouts emanate from the new loops and so the process continues, with increasing numbers of capillary tips being formed, until the new vessels penetrate the tumor.
6. In the stage of maturation, the newborn vessel is completed by the formation of new extracellular matrix and by the arrival of other cells named pericytes and sometimes of flat muscle cells. During this phase a major role is played by some molecules called angiopoietins leading to the development of the simple endothelial tubes into more elaborate vascular tree composed of several cell types. In fact, they

contribute to the maintenance of vessel integrity through the establishment of appropriate cell-cell and cell-matrix connections.

7. After the formation of the vascular network, a remodelling process starts. This involves the loss of some physiologically useless capillaries and the remodelling of the extracellular matrix. Shear stress and pressure inside the vessel are the most important drivers of the remodelling process.

At this point the tumor receives much more nutrient and the tumor cells become very aggressive with their mitotic rate increasing considerably leading to a much faster growth.

It has to be mentioned that mechanics has an important role not only in the formation and regression of blood vessel, but also on the interaction with the outer environment. For instance, growing around the vessel which is usually immature (Step 5 above), the tumor compresses it and might cause its collapse. In turn this makes the surrounding tissue hypoxic and leads to new stimulation of the angiogenic pathway above, so that the formation of new vessels and tumor growth is subject to a cyclic behavior.

### 3 Multiphase Models

Referring to Araujo and McElwain [6] for a recent review, we here recall that the first models dealing with avascular tumor growth worked under the hypotheses that the tumor is made by only one type of cells occupying a constant volume ratio  $\bar{\phi}_T$ , e.g. they fill the space as a bunch of rigid spheres in a close packing configuration, so that the mass balance equation

$$\rho \left[ \frac{\partial \phi_T}{\partial t} + \nabla \cdot (\phi_T \mathbf{v}_T) \right] = \rho \Gamma_T, \quad (3.1)$$

where  $\rho$  can be taken as the constant density of water, and  $\phi_T$  is the volume ratio occupied by tumor cells, can be written as

$$\bar{\phi}_T \nabla \cdot \mathbf{v}_T = \Gamma_T, \quad (3.2)$$

where  $\Gamma_T$  is a function of the concentration of nutrients and of a plethora of important chemical factors that are diluted in the extracellular liquid surrounding the cells and influence all vital functions of the tumor.

Enforcing a symmetry condition, usually spherical symmetry, allows to reduce the number of space variables to one and the velocity vector to a

scalar, so that one can directly integrate (3.2) to have the velocity in any point

$$v_T(r, t) = \frac{1}{r^2 \bar{\phi}_T} \int_0^r \Gamma_T(x, t) x^2 dx, \quad (3.3)$$

and, in particular, the evolution of the free border of the tumor

$$\frac{dR}{dt}(t) = v_T(R(t), t) = \frac{1}{R^2(t) \bar{\phi}_T} \int_0^{R(t)} \Gamma_T(x, t) x^2 dx. \quad (3.4)$$

The core of these type of models consisted then in describing how the growth term  $\Gamma_T$  depends on the chemical factors and nutrients diffusing in the environment. The evolution of the tumor border then is a by-product of the geometrical reasoning. In fact, Eq. (3.4) corresponds to a global mass balance on the tumor mass which determines how the tumor grows, without resorting to any force balance. In particular, nutrient limited radius can possibly be obtained by solving

$$\int_0^{R(t)} \Gamma_T(x, t) x^2 dx = 0, \quad (3.5)$$

which is related to a global balance between proliferation in the outer rim and death in the core. A similar consideration holds when including the existence of quiescent and necrotic regions in the tumor.

At this point, if the tumor is immersed in a homogeneous environment with known mechanical properties, then by knowing the (radial) displacement of the tumor border, one could compute the stress in the surrounding tissue.

As examined in [5], there were some difficulties in generalising this method to three-dimensional problems and to problems involving more populations. For this reasons, some years ago several authors (see, for instance, [14, 15, 20, 44, 45, 46, 53]) started linking, in the simplest possible way, motion to stress describing the tumor as a deformable porous material. Recently, the multiphase approach was described by Araujo and McElwain [7] for a general mixture of  $n$  constituents. In the following we will focus on specific applications referring to [5] and [7] for the general case.

### 3.1 A Basic Triphasic Model: ECM, Tumor Cells and Extracellular Liquid

As discussed above a tumor is at least made of three main constituents occupying a relevant percentage of space: tumor cells, extracellular matrix (ECM) and extracellular liquid. In addition one should consider the nutrients and chemical factors diffusing in the liquid and absorbed/produced

by the cells. However, in this section we will not focus on them but on the constituents filling the available space and present a very general tri-phasic model. After that, we will consider some special cases that will be applied in the following section to describe specific phenomena.

The starting point is to write the mass balance equations for the constituents

$$\frac{\partial \phi_0}{\partial t} + \nabla \cdot (\phi_0 \mathbf{v}_0) = \Gamma_0, \quad (3.6)$$

$$\frac{\partial \phi_T}{\partial t} + \nabla \cdot (\phi_T \mathbf{v}_T) = \Gamma_T, \quad (3.7)$$

$$\frac{\partial \phi_\ell}{\partial t} + \nabla \cdot (\phi_\ell \mathbf{v}_\ell) = \Gamma_\ell, \quad (3.8)$$

where  $\phi_0$ ,  $\phi_T$ , and  $\phi_\ell$  are the volume ratios occupied by ECM, tumor cells, and extracellular liquid, respectively, and  $\mathbf{v}_0$ ,  $\mathbf{v}_T$ , and  $\mathbf{v}_\ell$  are the relative velocities.

The saturation assumption implies that

$$\phi_0 + \phi_T + \phi_\ell = 1, \quad (3.9)$$

and if the mixture is closed, then the growth terms satisfy

$$\Gamma_0 + \Gamma_T + \Gamma_\ell = 0. \quad (3.10)$$

The momentum balance equations per constituent write

$$\rho \phi_0 \left( \frac{\partial \mathbf{v}_0}{\partial t} + \mathbf{v}_0 \cdot \nabla \mathbf{v}_0 \right) = \nabla \cdot \mathbf{T}_0 + \mathbf{b}_0 + \mathbf{m}_0^\sigma, \quad (3.11)$$

$$\rho \phi_T \left( \frac{\partial \mathbf{v}_T}{\partial t} + \mathbf{v}_T \cdot \nabla \mathbf{v}_T \right) = \nabla \cdot \mathbf{T}_T + \mathbf{b}_T + \mathbf{m}_T^\sigma, \quad (3.12)$$

$$\rho \phi_\ell \left( \frac{\partial \mathbf{v}_\ell}{\partial t} + \mathbf{v}_\ell \cdot \nabla \mathbf{v}_\ell \right) = \nabla \cdot \mathbf{T}_\ell + \mathbf{b}_\ell + \mathbf{m}_\ell^\sigma, \quad (3.13)$$

where  $\mathbf{T}_i$  is the partial stress tensor,  $\mathbf{b}_i$  is the body force and  $\mathbf{m}_i^\sigma$  is the interaction force acting on the  $i$ -th constituent due to its interaction with the other constituents.

Before proceeding we recall that in a Lagrangean frame of reference, (related to the constituent) the mass balance equations for the tumor cells can be written as

$$\frac{d}{dt}(\phi_T J_T) = \Gamma_T J_T, \quad (3.14)$$

where  $J_T = \det \mathbf{F}_T$  and  $\mathbf{F}_T$  is the deformation gradient relative to the tumor constituent. Similar relations hold for the other constituents. The meaning of Lagrangean will be discussed in the following.

The main contribution to the interaction forces can be assumed to be proportional to the velocity difference between the constituents. Compatibly with thermodynamics the saturation assumption implies the existence of a Lagrangean multiplier  $P$  which is then identified with the extracellular liquid pressure in the constitutive equations, so that one can write

$$\begin{aligned}
 \mathbf{m}_\ell^\sigma &= P\nabla\phi_\ell - \mathbf{M}_{\ell T}(\mathbf{v}_\ell - \mathbf{v}_T) - \mathbf{M}_{\ell 0}(\mathbf{v}_\ell - \mathbf{v}_0) \\
 &\quad - \frac{\Gamma_\ell}{2}\mathbf{v}_\ell + \frac{\Gamma_\ell - \Gamma_T}{6}\mathbf{v}_T + \frac{\Gamma_\ell - \Gamma_0}{6}\mathbf{v}_0, \\
 \mathbf{m}_T^\sigma &= P\nabla\phi_T - \mathbf{M}_{\ell T}(\mathbf{v}_T - \mathbf{v}_\ell) - \mathbf{M}_{T0}(\mathbf{v}_T - \mathbf{v}_0) \\
 &\quad - \frac{\Gamma_T}{2}\mathbf{v}_T + \frac{\Gamma_T - \Gamma_\ell}{6}\mathbf{v}_\ell + \frac{\Gamma_T - \Gamma_0}{6}\mathbf{v}_0, \\
 \mathbf{m}_0^\sigma &= P\nabla\phi_0 - \mathbf{M}_{T0}(\mathbf{v}_0 - \mathbf{v}_T) - \mathbf{M}_{\ell 0}(\mathbf{v}_0 - \mathbf{v}_\ell) \\
 &\quad - \frac{\Gamma_0}{2}\mathbf{v}_0 + \frac{\Gamma_0 - \Gamma_\ell}{6}\mathbf{v}_\ell + \frac{\Gamma_0 - \Gamma_T}{6}\mathbf{v}_T,
 \end{aligned} \tag{3.15}$$

where  $\mathbf{M}_{ij}$  refers to the interaction between the  $i$ -th and the  $j$ -th constituent and

$$\begin{aligned}
 \mathbf{T}_\ell &= -(P\phi_\ell)\mathbf{I} + \hat{\mathbf{T}}_\ell, \\
 \mathbf{T}_T &= -(P\phi_T)\mathbf{I} + \hat{\mathbf{T}}_T, \\
 \mathbf{T}_0 &= -(P\phi_0)\mathbf{I} + \hat{\mathbf{T}}_0,
 \end{aligned} \tag{3.16}$$

where  $\hat{\mathbf{T}}_i$  is named excess stresses. The terms in (3.15) proportional to the mass production rates  $\Gamma_i$  are however negligible, as discussed in [80].

In biological phenomena inertia can be neglected and also the interaction force between the extracellular matrix and the liquid is negligible (because in most cases the ECM has a fibrous structure filling a moderate amount of space) with respect to the interaction force between cell and liquid and above all cell and ECM. However, this last assumption is not essential and can be dropped.

In addition, as a first approximation we will consider the ECM as rigid. Under these assumptions one can simplify (3.6)–(3.8) and (3.11)–(3.13)

writing

$$\left\{ \begin{array}{l} \frac{\partial \phi_0}{\partial t} = \Gamma_0, \\ \frac{\partial \phi_T}{\partial t} + \nabla \cdot (\phi_T \mathbf{v}_T) = \Gamma_T, \\ \frac{\partial \phi_\ell}{\partial t} + \nabla \cdot (\phi_\ell \mathbf{v}_\ell) = \Gamma_\ell, \\ \mathbf{0} = -\phi_T \nabla P + \nabla \cdot \hat{\mathbf{T}}_T + \mathbf{b}_T + \mathbf{M}_{\ell T}(\mathbf{v}_\ell - \mathbf{v}_T) - \mathbf{M}_{T0} \mathbf{v}_T, \\ \mathbf{0} = -\phi_\ell \nabla P + \nabla \cdot \hat{\mathbf{T}}_\ell - \mathbf{M}_{\ell T}(\mathbf{v}_\ell - \mathbf{v}_T), \end{array} \right. \quad (3.17)$$

because the rigidity assumption implies that the stress tensor  $\mathbf{T}_0$  simply reacts to the forces applied to the ECM. The body force  $\mathbf{b}_T$  relates for instance to chemotactic or haptotactic action on the tumor cells, while  $\mathbf{b}_\ell$  is assumed to vanish.

If as usual in porous media model it is assumed that  $\hat{\mathbf{T}}_\ell = \mathbf{0}$ , the last equation gives rise to Darcy's law and can then more familiarly be written as

$$\mathbf{v}_\ell - \mathbf{v}_T = -\mathbf{K} \nabla P, \quad (3.18)$$

where  $\mathbf{K}$  is related to the permeability and is a function of the liquid volume ratio.

In order to eliminate the interaction force between the liquid and the cells, it might be convenient to add the two momentum equations to obtain

$$-(1 - \phi_0) \nabla P + \nabla \cdot \hat{\mathbf{T}}_T - \mathbf{K}_0^{-1} \mathbf{v}_T + \mathbf{b}_T = \mathbf{0}, \quad (3.19)$$

where  $\mathbf{K}_0 = \mathbf{M}_{T0}^{-1}$  is related to the permeability of the sticky granular flow in the porous structure constituted by the ECM network. This equation can then take the place of the first momentum equation in (3.17)

Hence the basic model can be written as

$$\left\{ \begin{array}{l} \frac{\partial \phi_0}{\partial t} = \Gamma_0, \\ \frac{\partial \phi_T}{\partial t} + \nabla \cdot (\phi_T \mathbf{v}_T) = \Gamma_T, \\ \nabla \cdot (\phi_T \mathbf{v}_T + \phi_\ell \mathbf{v}_\ell) = 0, \\ \mathbf{v}_\ell - \mathbf{v}_T = -\mathbf{K} \nabla P, \\ \mathbf{v}_T = \mathbf{K}_0 \left[ -(1 - \phi_0) \nabla P + \nabla \cdot \hat{\mathbf{T}}_T + \mathbf{b}_T \right], \end{array} \right. \quad (3.20)$$

where  $\phi_\ell = 1 - \phi_0 - \phi_T$  and (3.20)<sub>3</sub> was obtained by summing the mass balance equations and using (3.9) and (3.10).

### Limit Case: Neglecting the Mechanical Interaction with the Extracellular Liquid

Consider the case in which the permeability tensor is isotropic. If, for sake of simplicity,  $K_0 \gg K$ , as it is plausible, by substituting the gradient of pressure from Darcy's law (3.18) to (3.19), it can be readily realised that as a first approximation

$$\mathbf{v}_T = K_0 \left( \nabla \cdot \hat{\mathbf{T}}_T + \mathbf{b}_T \right). \quad (3.21)$$

We notice that if  $\mathbf{b}_T$  is proportional to the gradient of some chemical concentration

$$\mathbf{b}_T = \chi \nabla c, \quad (3.22)$$

and the partial stress tensor is neglected, Eq.(3.21) implies the usual chemotactic closure

$$\mathbf{v}_T = w \nabla c, \quad (3.23)$$

where  $w = K_0 \chi$ .

In particular, one has the classical chemotactic models

$$\frac{\partial \phi_T}{\partial t} + \nabla \cdot (w \phi_T \nabla c) = \Gamma_T. \quad (3.24)$$

Chemotaxis can then be conceived as a force balanced by the drag force exerted by the substratum and not as a convenient closure of the mass balance equation.

It is well known that Eq. (3.24) with the concentration either given or evolving according to a typical reaction-diffusion equation may be characterized by a solution that blows-up in finite time. On the other hand, Kowalczyk [60] showed that if mechanics is properly accounted for, i.e. if (3.21) is used with suitable constitutive equation for the stress the blow-up of the solution is prevented. For instance, it is enough to assume that the ensemble of cells behaves as an elastic fluid with a convex pressure-volume ratio dependence.

In the case of more chemotactic/haptotactic effects, one has the model

$$\begin{cases} \frac{\partial \phi_0}{\partial t} = \Gamma_0, \\ \frac{\partial \phi_T}{\partial t} + \nabla \cdot \left[ K_0 \phi_T \left( \nabla \cdot \hat{\mathbf{T}}_T + \sum_i \chi_i \nabla c_i \right) \right] = \Gamma_T, \end{cases} \quad (3.25)$$

which, of course, has to be associated with suitable reaction-diffusion equations for the chemical factors  $c_i$ .

The first equation describes the possible deposition or degradation of the extracellular matrix. If the stress tensor is isotropic,  $\hat{\mathbf{T}}_T = -\Sigma(\phi_T)\mathbf{I}$ , then (3.25)<sub>2</sub> may be re-written as

$$\frac{\partial \phi_T}{\partial t} + \nabla \cdot \left( \sum_i w_i \phi_T \nabla c_i \right) = \nabla \cdot (K_0 \phi_T \Sigma'(\phi_T) \nabla \phi_T) + \Gamma_T, \quad (3.26)$$

where  $\Sigma'$  is the derivative of  $\Sigma$  with respect to the volume ratio  $\phi_T$  and  $w_i = K_0 \chi_i$ .

### Limit case: Constant ECM

If we assume now that the amount  $\phi_0$  of ECM is maintained constant in the system, the first equation in (3.20) can be dropped. Substituting then  $\mathbf{v}_\ell$  from Darcy's law in the third equation one has that

$$\nabla \cdot ((1 - \phi_0) \mathbf{v}_T - \phi_\ell \mathbf{K} \nabla P) = 0, \quad (3.27)$$

$$\nabla \cdot ((1 - \phi_0) \mathbf{v}_\ell + \phi_T \mathbf{K} \nabla P) = 0. \quad (3.28)$$

In one-dimensional problems, this implies that cells move up the pressure gradient, while the extracellular liquid moves in the opposite direction, which is in agreement with the experimental results by Dorie et al. [38, 39] on the internalization of cells.

As the interstitial pressure is higher inside the tumor than at its outer boundary, cells move towards the center of the tumor and the extracellular liquid flows towards the boundary. A recirculation flow then forms: tumor cell near the center die due to nutrient deprivation and generate re-usable, extracellular fluid. This liquid flows to the boundary where it is taken up by proliferating cells, that are then internalized in the tumor.

In particular, in the limit of negligible amount of ECM, then the interaction term with the ECM drops and we can simplify the last equation in (3.20) as

$$-\nabla P + \nabla \cdot \hat{\mathbf{T}}_T + \mathbf{b}_T = \mathbf{0}, \quad (3.29)$$

which for particular constitutive equations will lead to the model proposed in Section 4.2.

---

## 4 Constitutive Equations

As usual, the modelling procedure above needs the specification of the constitutive equations describing the mechanical response to strain. This is not a standard step in this case because tumor cells are generated and die during the evolution. There is then a difficulty in defining a reference configuration and in using a Lagrangean coordinate system. In particular, also the meaning of deformation loses the immediate meaning it had in classical continuum mechanics when dealing with inert matter. In fact, when dealing with a growing tumor, with respect to what we should measure deformations? The material is always changing. That is why the concept of evolving natural configuration described several times in this book becomes very helpful.

Of course, the problem is circumvented if one can model the tumor as a fluid, because in this case it is possible to use an Eulerian approach. This is what was done in the first models developed in a multiphase framework.

An issue to keep in mind when formulating constitutive equations for living tissues and in particular tumors is what can be actually measured by biologists. In fact, testing the mechanical behavior of living tissues is much more difficult than for inert matter, and has not been done yet for tumors.

In the following we will present some examples of models of tumor growth using different constitutive equations.

### 4.1 Elastic Fluid: An Example Describing Contact Inhibition of Growth

Referring to Section 2.1, in this section we focus on the fact that when cells are in a crowded environment they sense the presence of other cells and their behavior then crucially depends on how they can stand the pressure (see Fig. 1). We then focus on how this can affect both mitosis and production of extracellular matrix and matrix degrading enzymes and in particular how a misperception of the compression state can generate hyperplasia, fibrosis, and tumor lesions.

Of course, we are well aware that cellular mechanotransduction is not the only cause of formation of hyperplasia and tumors and that chemical factors will operate to regulate the reproduction rates. However, we recall that the aim of this chapter is to describe the mechanical aspects of tumor growth and therefore we focus on what happens when the only thing that transforms a normal cell into an abnormal cell is how it senses and responds to the stress exerted on it.

Here the stress and therefore its influence on the evolution of the cell population occurs through three contributions: cell replication, the production of extracellular matrix and the release of matrix degrading enzymes.

The main aim is to show how an underestimation of the compression state of the local tissue and then of the subsequent stress which is exerted on a cell, can generate by itself a clonal advantage on the surrounding cells leading to the replacement and the invasion of the healthy tissue.

In order to do that the model in [30] focuses on the evolution of

- the volume ratio  $\phi_n$  occupied by normal cells;
- the volume ratio  $\phi_T$  occupied by tumor cells or more precisely by abnormal cells which will give rise to hyperplasia and dysplasia;
- the volume ratio  $\phi_m$  occupied by host extracellular matrix;
- the volume ratio  $\phi_M$  occupied by extracellular matrix produced by tumor cells, which is known to be structurally and chemically different from that produced by normal cells;
- the concentration  $c$  of matrix degrading enzymes, e.g., the plasminogen activators or matrix metalloproteinases.

In the following an important role will be played by the overall volume ratio occupied by cells and extracellular matrix

$$\psi = \phi_n + \phi_T + \phi_m + \phi_M. \quad (4.1)$$

and by its relation with the stress.

We assume that what makes the difference between a normal and a tumor cell stays in the growth term and in its dependence from the stress level.

Generalizing Eq. (3.25) to the populations above, one can then write

$$\left\{ \begin{array}{l} \frac{\partial \phi_m}{\partial t} = \Gamma_m, \\ \frac{\partial \phi_M}{\partial t} = \Gamma_M, \\ \frac{\partial \phi_n}{\partial t} + \nabla \cdot \left[ K_{0n} \phi_n \left( \nabla \cdot \hat{\mathbf{T}} + \chi_{nm} \nabla \phi_m + \chi_{nM} \nabla \phi_M \right) \right] = \Gamma_n, \\ \frac{\partial \phi_T}{\partial t} + \nabla \cdot \left[ K_{0T} \phi_T \left( \nabla \cdot \hat{\mathbf{T}} + \chi_{Tm} \nabla \phi_m + \chi_{TM} \nabla \phi_M \right) \right] = \Gamma_T, \end{array} \right. \quad (4.2)$$

In [30] the simplest constitutive equation is used and the ensemble of cell is described as an elastic fluid

$$\hat{\mathbf{T}} = -\Sigma \mathbf{I}, \quad (4.3)$$

where  $\Sigma$  vanishes below a value  $\psi_0$ , is increasing for  $\psi > \psi_0$  and tends to infinity at  $\psi = 1$ . Of course, treating the multicellular spheroid as a viscous fluid as shown in the following section would be easy to do, make the model closer to reality, and confer more stability to the solution.

Haptotactic effects are expressed in the last two term on the left hand side of Eqs. (4.2)<sub>3</sub> and (4.2)<sub>4</sub>, which with respect to the existing literature take into account of the different behavior of cells in the presence of the two kinds of ECM. In fact, cells preferentially adhere to normal ECM, whilst the ECM produced by the tumor cells favors their motility (and also their proliferation, although here this aspect is neglected as explained above). Hence, the coefficients  $\chi_{ij}$  and  $K_{0j}$  are allowed to be different and to depend on the overall volume ratio  $\psi$  defined in (4.1) and on the percentage of extracellular matrix  $\psi_m = \phi_m + \phi_M$ . There is, in fact, an optimal concentration of ECM. Motility decreases both at smaller contents of ECM because of the lack of substratum to move on and at larger contents of ECM because of the increase of adhesive sites (see [52, 75]). In addition, it vanishes for high values of the overall volume ratio  $\psi$  because of the occupation of space by the cells and by the ECM.

Contact inhibition of growth is modelled by [30] assuming that mitosis stops when the volume ratio (or the compression) overcomes a given threshold. Their assumption is that the threshold value for a tumor is slightly larger than the physiological one. Actually, it may even tend to infinity, meaning that the cells are completely insensitive to compression and continue replicating independently of the compression level.

Of course, the growth terms depend on other quantities, e.g. the amount of nutrient and growth factors, but, as already stated, in this section we will only focus on the possible role of stress on tumor invasion. In doing this we tacitly assume that all the constituents necessary to grow and undergo mitosis can be abundantly found in the extracellular liquid that is a passive constituent in the global mass balance equation.

We will then consider the following growth terms

$$\Gamma_i = [\gamma_i H_\sigma(\psi - \psi_i) - \delta_i(\psi)] \phi_i, \quad i = n, T. \quad (4.4)$$

In fact, not only growth but also apoptosis may be influenced by the compression level, as shown in [51].

In (4.4)  $H_\sigma(\psi - \psi_i)$  is a mollifier of the step function, which is at least continuous, is constantly equal to 1 for  $\psi$  smaller than the threshold value  $\psi_i$ , and vanishes for  $\psi > \psi_i + \sigma$ . According to the discussion above the threshold values  $\psi_n$  and  $\psi_T$  are such that  $\psi_n < \psi_T$ .

Coming back to the evolution of the extracellular matrix, it contains many macromolecules, including fibronectin, laminin and collagen, which are produced in a stress-dependent way by the cells and are degraded by MDEs [26, 68, 76, 86].

Hence the remodelling process is obtained assuming the following growth terms in (4.2)<sub>1</sub> and (4.2)<sub>2</sub>

$$\begin{aligned}\Gamma_m &= \mu_n(\Sigma)\phi_n - \nu c\phi_m, \\ \Gamma_M &= \mu_T(\Sigma)\phi_T - \nu c\phi_M.\end{aligned}\tag{4.5}$$

While it is known that the degradation by MDEs does not distinguish between the two types of ECM, in (4.5) the production coefficients of ECM by normal and tumor cells might be different, as occurs in the case of fibrosis and of many tumors.

Finally, active MDEs are produced (or activated) by the cells, diffuse throughout the tissue and undergo some form of decay (either passive or active). So one has to introduce the following reaction-diffusion equation governing the evolution of MDE concentration

$$\frac{\partial c}{\partial t} = \kappa \nabla^2 c + \pi_n(\Sigma)\phi_n + \pi_T(\Sigma)\phi_T - \frac{c}{\tau}.\tag{4.6}$$

The functions  $\pi_n$  and  $\pi_T$  model the production of active MDEs by normal and tumor cells, respectively, which might be different and certainly depend on the compression level.

Actually, in the following we want to focus on the effect of stress on growth. So, neglecting the effect of ECM and haptotaxis on cell motion the complete system of equations can be summarized as

$$\left\{ \begin{array}{l} \frac{\partial \phi_n}{\partial t} = \nabla \cdot [\phi_n K_0(\psi, \psi_m) \Sigma'(\psi) \nabla \psi] + \gamma_n H_\sigma(\psi - \psi_n) \phi_n - \delta_n(\psi) \phi_n, \\ \frac{\partial \phi_T}{\partial t} = \nabla \cdot [\phi_T K_0(\psi, \psi_m) \phi_T \Sigma'(\psi) \nabla \psi] + \gamma_T H_\sigma(\psi - \psi_T) \phi_T - \delta_T(\psi) \phi_T, \\ \frac{\partial \phi_m}{\partial t} = \mu_n(\Sigma) \phi_n - \nu c \phi_m, \\ \frac{\partial \phi_M}{\partial t} = \mu_T(\Sigma) \phi_T - \nu c \phi_M, \\ \frac{\partial c}{\partial t} = \kappa \nabla^2 c + \pi_n(\Sigma) \phi_n + \pi_T(\Sigma) \phi_T - \frac{c}{\tau}. \end{array} \right.\tag{4.7}$$

We mention that if initially the tumor fills a compact region of space  $\Omega$ , one then has a free boundary problem related to (4.7) with the interface

between tumor and normal tissue moving with the common velocity of the cells

$$\mathbf{n} \cdot \frac{d\mathbf{x}_T}{dt} = \mathbf{n} \cdot \mathbf{v} = -K_0(\psi, \phi_m + \phi_M) \Sigma'(\psi) \mathbf{n} \cdot \nabla \psi, \quad (4.8)$$

and with (4.7)<sub>2</sub> valid inside  $\Omega$  and (4.7)<sub>1</sub> outside it.

In addition continuity of stress and velocity enforce the following interface conditions

$$\phi_n = \phi_T, \quad \mathbf{n} \cdot \nabla \phi_n = \mathbf{n} \cdot \nabla \phi_T. \quad (4.9)$$

Still referring to [30] for more details, in the case of constant production of ECM and MDEs a homogeneous stationary solution is given by

$$\begin{aligned} \phi_n &= \hat{\phi}_n = \psi_n + H_\sigma^{-1} \left( \frac{\delta_n}{\gamma_n} \right) - M_n, & \phi_m &= M_n, \\ \phi_T &= 0, & \phi_M &= 0, \\ c &= \pi_n \tau \left[ \psi_n - M_n + H_\sigma^{-1} \left( \frac{\delta_n}{\gamma_n} \right) \right], \end{aligned} \quad (4.10)$$

where

$$M_n = \frac{\mu_n}{\nu \pi_n \tau}, \quad (4.11)$$

and

$$H_\sigma^{-1} \left( \frac{\delta_n}{\gamma_n} \right) \in (0, \sigma) \quad (4.12)$$

Symmetrically, another stationary solution is

$$\begin{aligned} \phi_n &= 0, & \phi_m &= 0, \\ \phi_T &= \hat{\phi}_T = \psi_T - M_T + H_\sigma^{-1} \left( \frac{\delta_T}{\gamma_T} \right), & \phi_M &= M_T, \\ c &= \pi_T \tau \left[ \psi_T - M_T + H_\sigma^{-1} \left( \frac{\delta_T}{\gamma_T} \right) \right], \end{aligned} \quad (4.13)$$

where

$$M_T = \frac{\mu_T}{\nu \pi_T \tau}. \quad (4.14)$$

By a simple linear stability analysis with respect to homogeneous perturbations it can be proved that the former configuration is unstable with an exponential growth rate for the tumor population equal to

$$\gamma_T H_\sigma \left( \psi_n - \psi_T + H_\sigma^{-1} \left( \frac{\delta_n}{\gamma_n} \right) \right) - \delta_T. \quad (4.15)$$

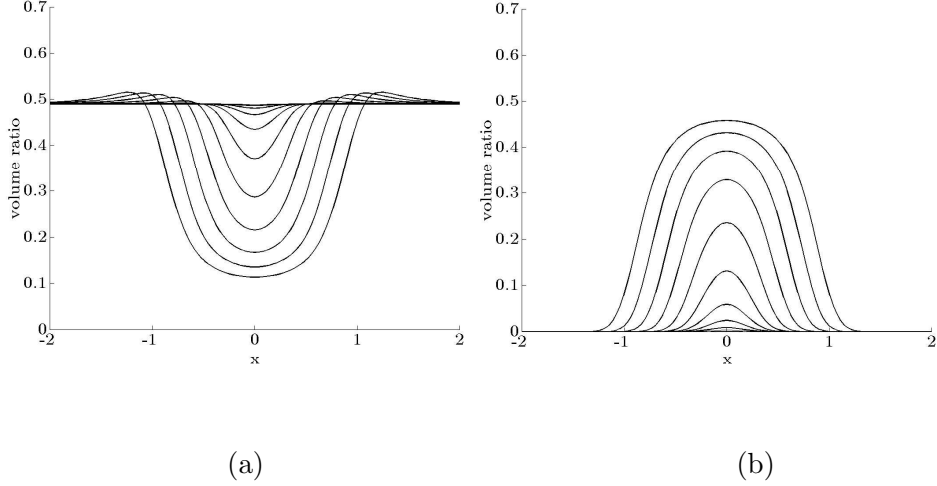


Figure 4: Early development of a tumor. Replacement of normal cells (left) by tumor cells (right) at times  $\tilde{t} = \gamma t = 1, \dots, 10$  without compression till  $\tilde{t} \approx 5$  and progressive compression of the surrounding tissue for larger times. But for  $\psi_n = 0.6$  and  $\psi_T = 0.7$ , the same parameters are used for both tumor and normal tissue  $\delta/\gamma = 0.1$ ,  $\mu = 0.1 \text{ days}^{-1}$ ,  $\pi/c_0 = 400 \text{ days}^{-1}$ ,  $\nu c_0 = 0.25 \text{ days}^{-1}$ ,  $\gamma\tau = 0.005$ ,  $\pi/c_0 = 400 \text{ days}$ ,  $M_0 = 0.2$ ,  $\sigma = 0.1$ , and  $a_0(x) = 0.001 \exp\{-30\tilde{x}^2\}$  where distances are scaled with  $\sqrt{\gamma/KE}$ .

Since tumor cells are characterised by a smaller sensitivity to compression (i.e.,  $\psi_n < \psi_T$ ,  $\delta_n = \delta_T$ ,  $\gamma_n = \gamma_T$ ), or a smaller apoptotic rate (i.e.,  $\delta_T < \delta_n$ ,  $\psi_n = \psi_T$ ,  $\gamma_n = \gamma_T$ ), or a larger growth rate (i.e.,  $\gamma_T > \gamma_n$ ,  $\psi_n = \psi_T$ ,  $\delta_n = \delta_T$ ), then

$$\psi_n + H_\sigma^{-1} \left( \frac{\delta_n}{\gamma_n} \right) < \psi_T + H_\sigma^{-1} \left( \frac{\delta_T}{\gamma_T} \right). \quad (4.16)$$

In order to describe in more details what happens in the early stages, consider the case in which all parameters for normal and tumor cells are equal but for  $\psi_T > \psi_n + H_\sigma^{-1}(\delta/\gamma)$  (we dropped the indexes to stress the equality).

Still referring to [30] for more details, if we assume that at a certain instant, considered as the initial time, some normal cells undergo some genetic mutation that makes them less sensitive to the compression level, so that, for instance,  $\phi_T(t=0, \mathbf{x}) = a_0(\mathbf{x})$ , then at early times one has the solution

$$\phi_T(t, \mathbf{x}) = a_0(\mathbf{x})e^{(\gamma-\delta)t} \quad (4.17)$$

$$\phi_M(t, \mathbf{x}) = \frac{a_0(\mathbf{x})}{\frac{\gamma-\delta}{\mu} + \frac{\psi_n}{M} - 1} \left[ e^{(\gamma-\delta)t} - e^{-\nu c_0 t} \right], \quad (4.18)$$

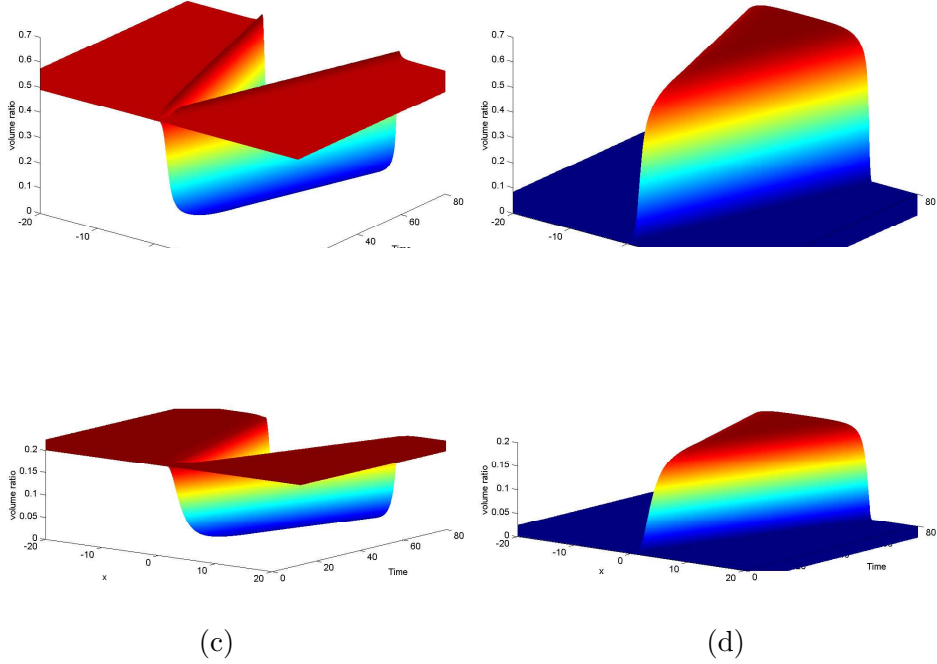


Figure 5: Tissue invasion for longer times and for the same parameters used in Fig. 4. The travelling wave characteristic and the transition layer are evident. The compression of the normal tissue due to the expansion of the hyperplasia is also put in evidence by the peaks in (a) corresponding to the normal tissue. (b) refers to the tumor tissue, (c) to the ECM produced by the normal tissue and (d) by that produced by the tumor.

and

$$\phi_n(t, \mathbf{x}) = \psi_n - M + H_\sigma^{-1} \left( \frac{\delta}{\gamma} \right) - \phi_T(t, \mathbf{x}), \quad (4.19)$$

$$\phi_m(t, \mathbf{x}) = M - \phi_M(t, \mathbf{x}), \quad (4.20)$$

$$c(t, \mathbf{x}) = \pi\tau \left[ \psi_T - M + H_\sigma^{-1} \left( \frac{\delta}{\gamma} \right) \right], \quad (4.21)$$

with  $M = M_n = M_T$ .

In particular, we stress that  $\phi_n(t, \mathbf{x}) + \phi_T(t, \mathbf{x})$ ,  $\phi_m(t, \mathbf{x}) + \phi_M(t, \mathbf{x})$ , and  $c(t, \mathbf{x})$  remain constant, which implies  $\Sigma'(\psi) = 0$  and absence of motion. For this reason, in [30] this phase is called relaxed replacement phase. In fact, tumor cells simply substitute normal cells without causing any compression of the tissue, as shown by the early development in Fig. 4a for  $\gamma t > 5$  and Fig. 5a.

A similar behavior can be shown if the production rates are stress dependent.

We observe that if  $a_0(\mathbf{x})$  has a compact support, as it should be because the source of the tumor is localized, then the solution for  $\phi_T$  will always have a compact support, since (4.7)<sub>2</sub> is parabolic degenerate.

After a time that can be estimated by

$$t \approx \frac{1}{\gamma - \delta} \log \left[ \frac{\delta \psi_n - M + H_\sigma^{-1} \left( \frac{\delta}{\gamma} \right)}{\gamma \max a_0(\mathbf{x})} \right], \quad (4.22)$$

the amount of tumor cells produced is larger than the amount of normal cells that would normally die. The tumor then start compressing the tissue, as observed experimentally, and the growth of the hyperplasia is accompanied by a compression of the normal tissue near the interface separating the two tissues shown by the maxima in Figs. 4a and 5a.

Cells start moving away from the compressed regions. At the same time the ECM is completely replaced by that produced by the tumor.

From Fig. 5 it is evident that the tumor front travels with a constant velocity. Of course, in the model the influence of nutrients is neglected, so from the biological point of view this makes sense till one can assume that the nutrients are abundantly supplied to the entire tumor. Including nutrients and starvation to the model would lead to nutrient limited growth as we shall see in the following section.

In [30] it is shown that the speed of the travelling wave solution can be evaluated as

$$v \approx \sqrt{2K_0 \Sigma'(\psi_n) \delta \left( 1 - \frac{\delta}{\gamma} \right) (\psi_T - \psi_n)}, \quad (4.23)$$

(if  $\psi_T = (1 + \epsilon)\psi_n$  with  $\epsilon \ll 1$ ) and there is a transition layer between the normal and abnormal tissue having width

$$z_2 - z_1 \approx \sqrt{\frac{2K_0 \Sigma'(\psi_n) (\psi_T - \psi_n)}{\delta \left( 1 - \frac{\delta}{\gamma} \right)}}. \quad (4.24)$$

In fact, to second order one has that

$$\begin{aligned} \phi_T &\approx \hat{\phi}_T - \frac{\gamma - \delta}{2KE} (z - z_1)^2 & \text{for } z \in [z_1, 0], \\ \phi_n &\approx \hat{\phi}_n + \frac{\delta}{2KE} (z - z_2)^2 & \text{for } z \in [0, z_2], \end{aligned} \quad (4.25)$$

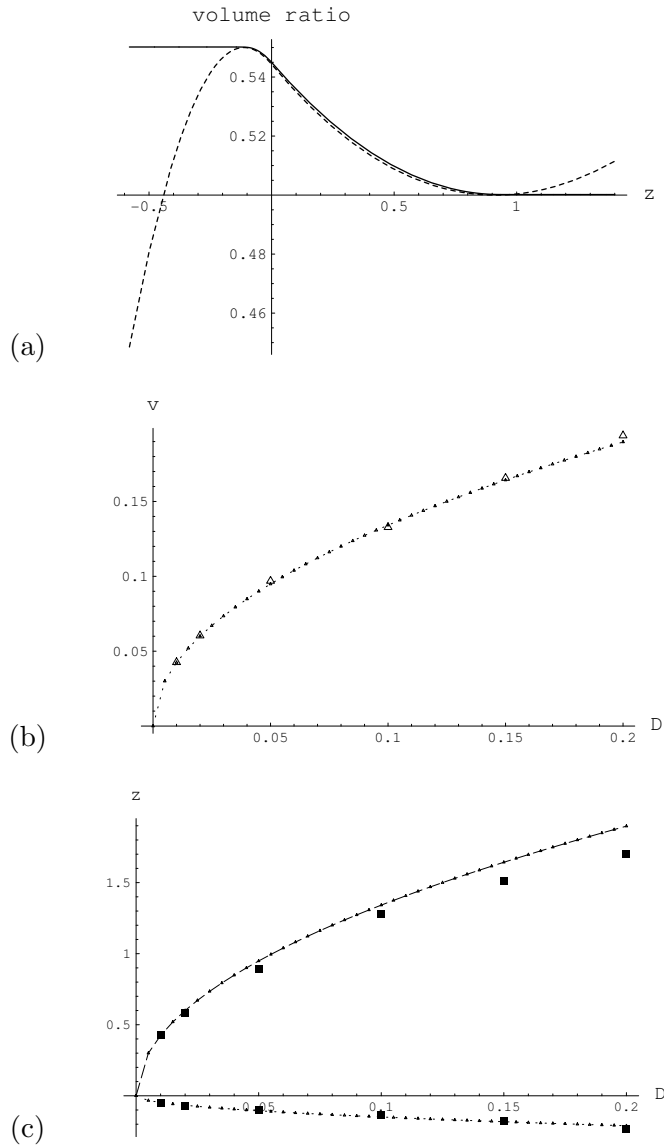


Figure 6: Travelling wave solution for  $\delta/\gamma = 0.1$ . In (a) comparison between analytical approximation (dotted line) and numerical solution (full line) for  $\psi_n = 0.5$  and  $\psi_T = 0.55$ . Negative  $z$ 's correspond to the tumor, positive  $z$ 's to the host tissue. Distances are scaled with  $z = \sqrt{\gamma/KE}x$ . (b) Velocity of propagation as a function of  $D = \psi_T - \psi_n$ . Analytical estimates are given by the curves and numerical results by the squares. In (c) The lower curves refer to  $z_1$  and the upper curves to  $z_2$ . The thickness of the transition layer is then given by the distance between the two curves.

where  $\hat{\phi}_n$  and  $\hat{\phi}_T$  are respectively defined in (4.10) and (4.13) and

$$z_1 \approx -\frac{v}{\gamma - \delta}, \quad z_2 \approx \frac{v}{\delta}. \quad (4.26)$$

Figure 6a shows a comparison between the travelling wave solution (4.25) and the one obtained numerically, while Figures 6b,c compare the theoretical values of  $v$ ,  $z_1$ ,  $z_2$ , and then of the transition layer thickness  $z_1 + z_2$  with those obtained from the simulations.

As mentioned in Section 2.2 (see also Table 1), often tumors are characterized by a considerable change in the content of ECM. In fact, for instance, self-palpation is encouraged in order to identify possible breast tumors by sensing a stiffer nodule with respect to the surrounding tissue. Figure 7 reports what happens if  $\mu_T > \mu_n$ , corresponding to the generation of fibrotic tissue, with a smaller amount of cells and a compressed tissue (see Fig. 7e).

In this case the normal ECM is produced by the cells at a rate larger than physiological, so that at the end the hyperplastic tissue replacing the normal one is also characterised by a larger amount of ECM. In particular, doubling the rate of ECM production leads to a fibrotic tissue with a ratio of cells versus ECM content nearly equal to 1.02, compared with 2.45 in the physiological situation. A similar thing is obtained halving the rate of production of MDEs.

On the other hand, a hypo-production of ECM (or a hyper-production of MDEs) leads to a tissue characterised by a ratio of cells versus ECM content nearly equal to 6.86 as shown in Fig. 8 with a larger amount of cells and a smaller amount of ECM (see Fig. 1a).

Comparing Figs. 7e and 8e, one can notice that in the two situations the overall volume ratio  $\psi$  is very similar. However, the composition of the tissue is dramatically different with the obvious changes in the mechanical properties of the tissue. This is due to the fact that the overall volume ratio is mainly influenced by the value at which growth stops while the tissue composition is influenced by the other parameters. A similar thing would occur by a pathological production of MDEs.

## 4.2 Viscous Fluid: An Example Showing Nutrient Limited Growth

In this section, following [20], we will assume that the solid constituent of the mixture can be modeled as an ensemble of sticky cells floating in a liquid environment and neglecting the presence of ECM.

In [20] the ensemble of cells is described as a “viscous growing fluid”, so that also in this case one does not need to consider the deformations of the material with respect to some reference configuration, but only to deal with their rates. In this respect, it is possible to use an Eulerian framework

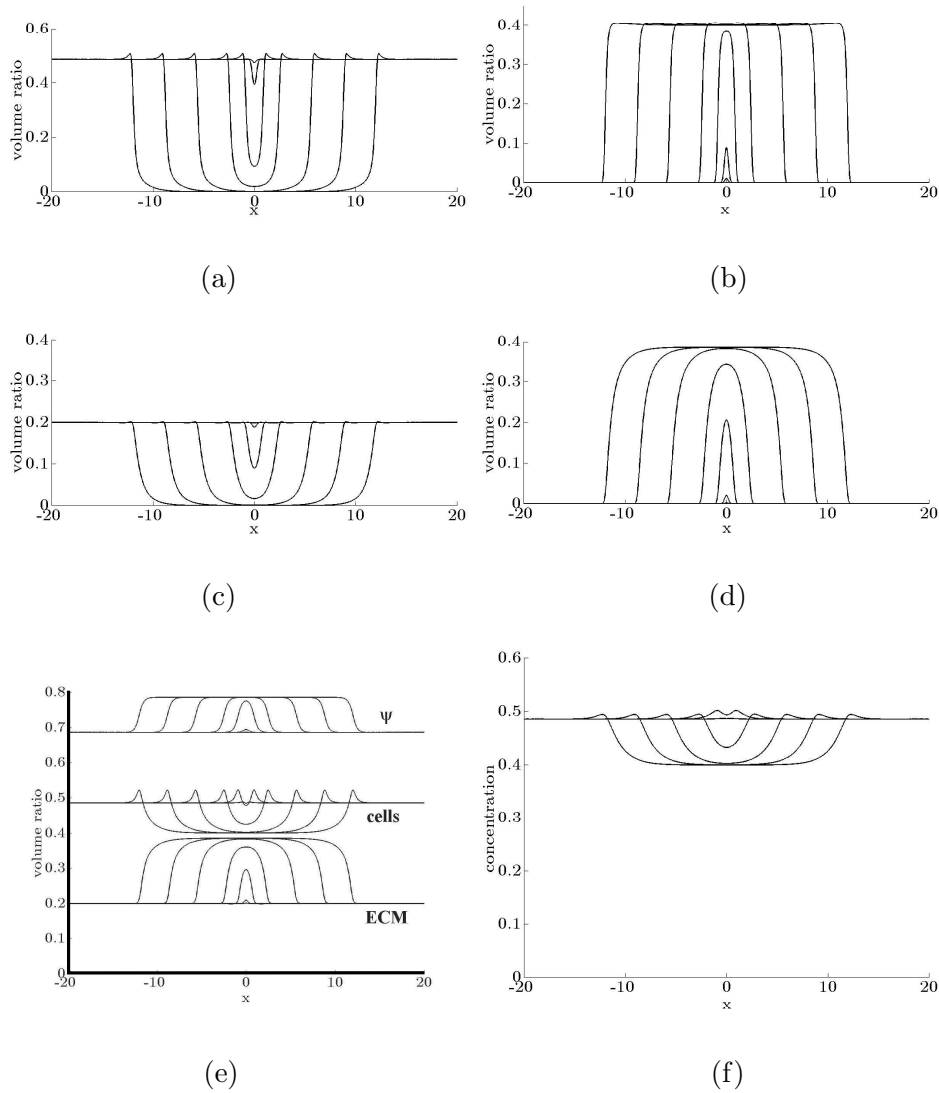


Figure 7: Formation of fibrosis for  $\mu_T = 0.2 \text{ days}^{-1}$ , with all other parameters as in Fig. 4 and at times  $\tilde{t} = \gamma t = 0, 2.5, 5, 10, 20, 40, 60, 80$ . Volume ratio of normal cells (a) and tumor cells (c) and ECM produced by normal cells (b) and by tumor cells (d). In (e) the lower set of curves refer to the volume ratio of ECM  $\psi_m = \phi_m + \phi_M$ , the central ones to the volume ratio of cells  $\phi_n + \phi_T$ , and the upper ones to the overall volume ratio  $\psi$ , i.e. the sums of the two above. In (f) the concentration of MDEs.

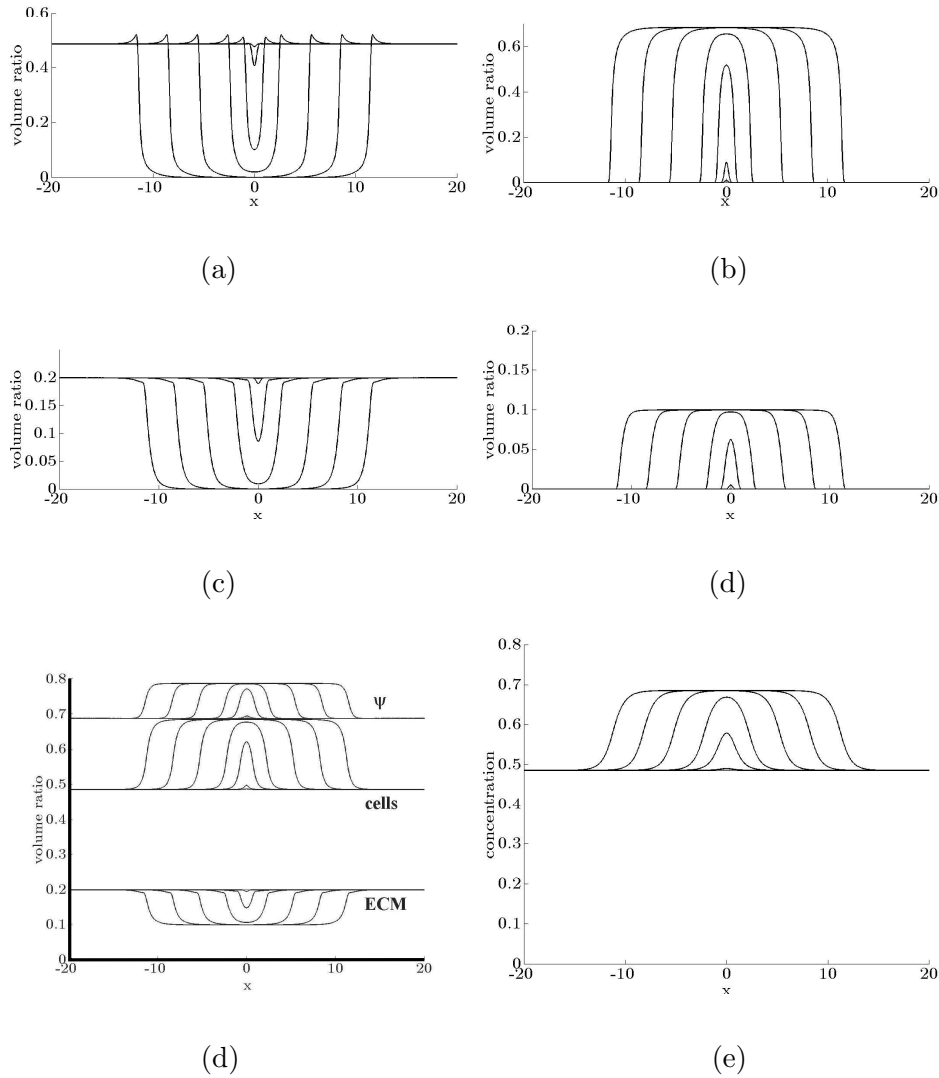


Figure 8: Hypo-production of ECM for  $\mu_T = 0.05 \text{ days}^{-1}$ , with all other parameters as in Fig. 4 and at times  $\tilde{t} = \gamma t = 0, 2.5, 5, 10, 20, 40, 60, 80$ . Volume ratio of normal cells (a) and tumor cells (c), of ECM produced by normal cells (b) and by tumor cells (d). In (e) The lower set of curves refer to the volume ratio of ECM  $\psi_m = \phi_m + \phi_M$ , the central ones to the volume ratio of cells  $\phi_n + \phi_T$ , and the upper ones to the overall volume ratio  $\psi$ , i.e. the sums of the two above. In (f) the concentration of MDEs.

and the mathematical description of the “growing fluid” just involves an additional source of mass.

To complete the picture we might consider also  $N$  chemical factors and nutrients diffusing in the extracellular liquid

$$\frac{\partial c_i}{\partial t} + \nabla \cdot (c_i \mathbf{v}_\ell) = \nabla \cdot (k_i \nabla c_i) + \gamma_i \phi_T - \delta_i \phi_T c_i, \quad i = 1, \dots, N, \quad (4.27)$$

where the last two terms refer respectively to the possible production and absorption by tumor cells and  $\gamma_i$  and  $\delta_i$  might not be constant.

Actually, in [20] only a general nutrient  $n$  perfusing through the vessels far away from the tumor and absorbed by the cells is considered, so that just the equation

$$\frac{\partial n}{\partial t} + \nabla \cdot (n \mathbf{v}_\ell) = \nabla \cdot (k_n \nabla n) - \delta_n \phi_T n, \quad (4.28)$$

need be added to (3.20) with  $\mathbf{b}_T = \mathbf{0}$  and

$$\hat{\mathbf{T}}_T = (-\Sigma + \lambda_T \nabla \cdot \mathbf{v}_T) \mathbf{I} + 2\mu_T \mathbf{D}_T, \quad (4.29)$$

where  $\mathbf{D}_T = (\nabla \mathbf{v}_T + \nabla \mathbf{v}_T^T)/2$  is the rate of strain tensor. It must be stressed that neither  $\lambda_T$  nor  $\mu_T$  will be constant as viscous forces among cells increase, at least linearly, with their volume ratio. Of course, as in the previous section, also  $\Sigma$  is a function of the volume ratio measuring the response to compression and is taken positive in compression.

The growth term  $\Gamma_T$  is constructed in [20] on the basis of the following phenomenological observations:

- Proliferation occurs if the nutrient concentration exceeds the threshold value  $\hat{n}$ . Where  $n (> \hat{n})$  is close to  $\hat{n}$  the proliferation rate is proportional to  $n - \hat{n}$ ; as  $n$  increases, the proliferation rate eventually saturates.
- Cell proliferation is strongly affected by the presence of other cells which exert stress on the membrane of the replicating cell. In particular, the proliferation rate approaches zero as the volume ratio approaches one.
- Apoptosis is proportional to the volume ratio of cells.

A suitable function  $\Gamma_T$ , which combines these features and is continuous across  $n = \hat{n}$ , is given by:

$$\Gamma_T = \frac{\gamma \phi_T}{1 + \sigma \Sigma(\phi_T)} \frac{(n - \hat{n})_+}{1 + \nu n} - \delta \phi_T, \quad (4.30)$$

where  $(f)_+$  is the positive part of  $f$ . Hence, when

$$\frac{(n - \hat{n})_+}{1 + \nu n} < \frac{\delta}{\gamma} [1 + \sigma \Sigma(\phi_T)], \quad (4.31)$$

there is a net loss of cells which at the end will lead to a limit radius related to the amount of nutrient available.

The stress-volume ratio relation is obtained in [20] under the following considerations

- Two cells which are far apart ignore each other;
- If the distance between two cells falls below a threshold value then they attract each other;
- When cells in contact are pulled apart, an adhesive force competes with cell separation;
- If two cells are too close together, they experience a repulsive force;
- The repulsive force becomes infinite in the limit as the cells are packed so densely that they fill the whole control volume.

In the one-dimensional case, the previous description can be reformulated as follows:

- Cell in regions where  $\phi_T < \hat{\phi}$  experience neither attractive nor repulsive forces;
- The attractive force attains a maximum value ( $\Sigma = \Sigma_1$ ) when  $\phi_T = \phi_1 > \hat{\phi}$ ;
- The attractive and repulsive forces balance when  $\phi_T = \phi_2 > \phi_1$
- The repulsive force becomes infinite as  $\phi_T$  tends to one.

It has to be mentioned that a continuous function satisfying the properties above would be decreasing in the interval  $(\hat{\phi}, \phi_1)$ , giving rise to a problem which might become ill-posed (see Eq.(4.35) below), if the solution achieves values in the interval above, giving rise to dramatic instability problems. However, Witelski [97] showed that a shock layer forms corresponding to “a quick jump over the bad section ... where the diffusion coefficient is negative” (see also [40]). Hence if one start from initial conditions away from  $(\hat{\phi}, \phi_1)$  the solution never achieves values in that interval, but the solution might lose regularity by forming a sharp front more or less like in phase transition problems. However, having in mind the experiments discussed in Section 4.4 and sketched in Fig. 13, one can also

assume that the multicell spheroid fractures for  $\phi_T < \phi_1$  under the action of tensile stresses, keeping the validity of the model for  $\phi_T > \phi_1$  where  $\Sigma(\phi_T)$  is increasing.

We finally mention that the Young modulus for a tumor is of the order of 1 kPa (see Table 2), while, as will be discussed in Section 4.4, the maximum tension is of the order of 0.1 kPa [10].

Summarizing, recalling (3.20), one has

$$\left\{ \begin{array}{l} \frac{\partial \phi_T}{\partial t} + \nabla \cdot (\phi_T \mathbf{v}_T) = \frac{\gamma \phi_T}{1 + \sigma \Sigma(\phi_T)} \frac{(n - \hat{n})_+}{1 + \nu n} - \delta \phi_T, \\ \nabla \cdot (\phi_T \mathbf{v}_T + \phi_\ell \mathbf{v}_\ell) = 0, \\ \nabla P = -\Sigma' \nabla \phi_T + \nabla (\lambda_T \nabla \cdot \mathbf{v}_T) + \nabla \cdot [\mu_T (\nabla \mathbf{v}_T + (\nabla \mathbf{v}_T)^T)], \\ \frac{\partial n}{\partial t} + \nabla \cdot (n \mathbf{v}_\ell) = \nabla \cdot (k_n \nabla n) - \delta_n \phi_T n, \end{array} \right. \quad (4.32)$$

where  $\mathbf{v}_\ell$  is given by Darcy's law

$$\mathbf{v}_\ell = \mathbf{v}_T - K \nabla P. \quad (4.33)$$

The growth problem is a free-boundary problem with a material interface fixed on the tumor cells. This interface moves with the cell velocity

$$\mathbf{n} \cdot \frac{d\mathbf{x}_T}{dt} = \mathbf{n} \cdot \mathbf{v}_T. \quad (4.34)$$

An interesting simplification occurs in one-dimensional problems with viscous contributions neglected. In this case, the system reduces to

$$\frac{\partial \phi_T}{\partial t} = \frac{\partial}{\partial x} \left( K \Sigma' \phi_T \frac{\partial \phi_T}{\partial x} \right) + \Gamma_T, \quad (4.35)$$

$$\frac{\partial n}{\partial t} + \frac{\partial}{\partial x} \left( \frac{\hat{K} \Sigma' \phi_T}{1 - \phi_T} \frac{\partial \phi_T}{\partial x} n \right) = k_n \frac{\partial^2 n}{\partial x^2} - \delta_n \phi_T n, \quad (4.36)$$

with

$$v_T = -\phi_\ell K \Sigma' \frac{\partial \phi_T}{\partial x}, \quad (4.37)$$

$$v_\ell = \phi_T K \Sigma' \frac{\partial \phi_T}{\partial x}, \quad (4.38)$$

and  $P + \Sigma = \text{constant}$ . In particular, Eq.(4.35) is similar to the equation encountered in many one-dimensional poro-elastic problems.

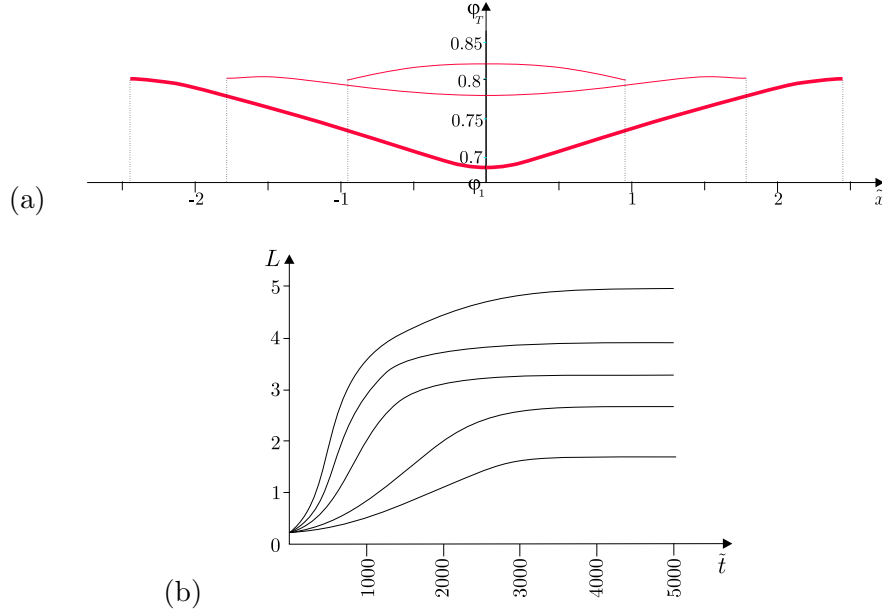


Figure 9: Evolution toward the steady state (thicker line) for  $\delta/\delta_n = 0.001$ , and  $\sigma = 0$ . In (a) the volume ratio is plotted versus space ( $\tilde{x} = \sqrt{\delta_n/\kappa_n}x$ ) for  $\tilde{\gamma} = \gamma n_{\text{ext}}/\delta_n = 0.0125$ . Transient times are  $\tilde{t} = \delta_n t = 500, 1000$ . In (b) the temporal evolution of the tumor size is given for different values of  $\tilde{\gamma} = 0.0025, 0.005, 0.0075, 0.01, 0.0125$  (from lower to upper curve).

Figure 9a describes the trend toward the stationary state and then how nutrient limits the growth of avascular tumors. Initially a stress-free tumor of size  $L = 0.1$  is implanted. We observe that at  $\tilde{t} = 500$  the tumor is still so small that all cells have sufficient nutrient to replicate (i.e.,  $n > \hat{n}$  everywhere). The maximum cell compaction occurs at the tumor center and, due to the repulsive forces they experience, cells move toward the border, causing the tumor to increase in size. At  $\tilde{t} = \delta_n t = 1000$  the nutrient concentration near the center of the tumor falls below  $n_0$  and cells there start dying. The location of the maximum cell volume fraction moves toward the tumor boundary, while in the center a (local) minimum appears. Cells which are located in the central region of the tumor, between the two symmetric maxima, move toward the center, whereas those in the outer regions, between the maxima and the tumor boundary, move toward the boundary. Of course, the tumor still grows, but at a reduced rate. In the stationary configuration (the lowest curve) the maximum cell volume fraction occurs on the tumor boundary. For the choice of parameters in the figure, at equilibrium the nutrient concentration at the tumor center only just exceeds that which triggers central necrosis and the formation of

a sharp front dividing the compact tumor from the necrotic core.

Figure 9b shows the temporal evolution of the tumor size for different values of growth rate  $\tilde{\gamma} = \gamma n_{\text{ext}}/\delta n$  where  $n_{\text{ext}}$  is the amount of nutrient at the tumor border.

Another result of the model is that as the cell proliferation rate decreases more rapidly with increasing cellular stress, the equilibrium tumor size becomes smaller and the cells more uniformly distributed across the tumor. Actually, in [20] it is shown that if this influence is sufficiently large then no nontrivial equilibrium solutions exist and the tumor is eliminated. From the application viewpoint, this suggests that if there were a method to make tumor cells more sensible to mechanical compression e.g. making its mitotic or apoptotic rate depend on the stress, this could be used to control the size of the tumor.

The following viscous-type constitutive equation

$$\mathbf{T} = -P\mathbf{I} + 2\mu_T \left[ \mathbf{D}_T - \frac{1}{3}(\nabla \cdot \mathbf{v}_T)\mathbf{I} \right], \quad (4.39)$$

has been also used by Franks and coauthors [44, 45, 46] under the additional strong hypothesis that all constituents filling the space move with the same velocity (live tumor cells and what they call surrounding material in [46], with the addition of death tumor cells in [44, 45]). In fact, the stress in (4.39) probably refers to the mixture. For instance, the model in [45], which describes tumor growth in a breast duct and also focuses on the mechanical interaction with the duct walls, writes in the notation of this chapter as

$$\left\{ \begin{array}{l} \frac{\partial \phi_T}{\partial t} + \nabla \cdot (\phi_T \mathbf{v}) = [An - B(1 - \delta n)]\phi_T, \\ \frac{\partial \phi_D}{\partial t} + \nabla \cdot (\phi_D \mathbf{v}) = B(1 - \delta n)\phi_T, \\ \frac{\partial \phi_\ell}{\partial t} + \nabla \cdot (\phi_\ell \mathbf{v}) = 0, \\ \frac{\partial n}{\partial t} + \nabla \cdot (n\mathbf{v}) = D\nabla^2 n - \gamma An\phi_T, \\ \nabla P = \mu \left[ \nabla^2 \mathbf{v} + \frac{1}{3}\nabla(\nabla \cdot \mathbf{v}) \right], \end{array} \right. \quad (4.40)$$

where  $\phi_D$  is the volume ratio of dead cells, which is joined with the constitutive equation (4.39) and the saturation assumption  $\phi_T + \phi_D + \phi_\ell = 1$ . The mixture is not closed, so that the global volume of the tumor is increased by the source term  $An$ . For sake of completeness, we mention that in [44] and [46] the Authors also add diffusion terms to the first three equations in (4.40).

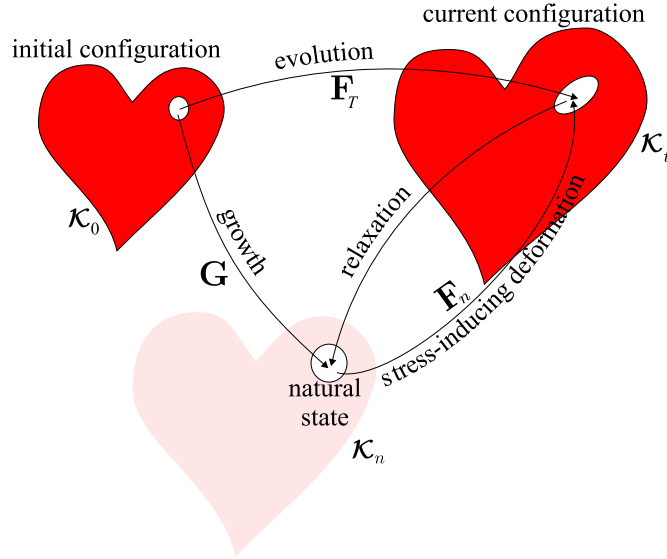


Figure 10: Evolving natural configuration. Notation

### 4.3 Evolving Natural Configurations in Tumor Growth

In the previous sections we have described some models that use fluid-like constitutive equations. However, this is only a rough approximation, because tumors as most tissue show solid-like characteristics. As already mentioned several times in this book, in this case in order to define, for instance, an elastic mechanical response, one needs to measure the deformation with respect to some reference state. However, the basic question is: “Deformation with respect to what, if the tissue is always changing?”

In order to address this problem Ambrosi and Mollica [3, 4] used the theory of evolving natural configurations splitting the evolution in growth and elastic deformation. In their model the interaction with the ECM and with the extracellular liquid are neglected and the tumor is described as a one-constituent compressible elastic body.

The theory for materials with evolving natural configurations is an ideal setting to investigate tumor growth as the growth of other tissues. In fact, the essential difficulty in formalizing the dynamics of growth is to model simultaneously the change in mass, and the stresses that accompany it, possibly caused by growth itself or by the application of external loads.

With the theory for materials with evolving natural configurations one is able to separate such contributions and to model each of them individually.

Following the notation in Fig. 10, the aim is then to distinguish in the evolution of the tumor given through the deformation gradient  $\mathbf{F}_T$  the contribution of pure growth from the stress-inducing deformation. In

particular, it is natural to work so that no growth occurs during stress-inducing deformation. By the way, from the biological point of view, the two contributions could be easily testable in principle as growth occurs on a much longer time scale (hours up to a day) than deformation.

The deformation gradient  $\mathbf{F}_T$  is a mapping from a tangent space onto another tangent space, and therefore it indicates how the body is deforming locally in going from  $\mathcal{K}_0$  to  $\mathcal{K}_t$ . Working in the tangent space, take a neighborhood of a point and assume to relieve its state of stress keeping its mass constant, so that it is allowed to relax to a stress-free configuration. The atlas of these configuration forms a natural configuration relative to  $\mathcal{K}_t$  which we denote by  $\mathcal{K}_n$ . Of course, this natural configuration depends on time. We will identify this deformation without growth with the tensor  $\mathbf{F}_N$ , which then describes how the body is deforming locally in going from the natural configuration  $\mathcal{K}_n$  to  $\mathcal{K}_t$ . The tensor

$$\mathbf{G} \equiv \mathbf{F}_N^{-1} \mathbf{F}_T, \quad (4.41)$$

tells how the body is growing locally.

Hence, the following decomposition holds

$$\mathbf{F}_T = \mathbf{F}_N \mathbf{G}. \quad (4.42)$$

The tensor  $\mathbf{F}_N$  is then connected to the stress response of the tumor to deformations while the tensor  $\mathbf{G}$  is the one that is directly connected to growth and will be therefore named growth tensor.

There are then two things to determine constitutively, how the natural configurations evolve, i.e., characterizing the growth tensor  $\mathbf{G}$ , and how the material behaves from each natural configuration.

Being the density of a single cell equal to the density of water, we will assume that for any given ‘‘particle’’ the volume ratio in the natural configuration and in the original reference configuration are the same, i.e.  $\phi_T(t=0) = \phi_N$ . Denoting by  $dV$ ,  $dV_N$ , and  $dv$  the volume elements in the reference, natural and current configuration, respectively, the related masses are then  $dM = \rho \phi_N dV$ ,  $dm = \rho \phi_N dV_N$ , and  $dm = \rho \phi_T dv$ . Since mass is preserved between  $\mathcal{K}_n$  and  $\mathcal{K}_t$ , one then has that

$$J_g = \det \mathbf{G} = \frac{dV_N}{dV} = \frac{dm}{dM}, \quad (4.43)$$

$$J_T = \det \mathbf{F}_T = \frac{dv}{dV} = \frac{\phi_N}{\phi_T} \frac{dm}{dM}, \quad (4.44)$$

and, in particular, because of (4.42),

$$J_N = \det \mathbf{F}_N = \frac{\phi_N}{\phi_T}. \quad (4.45)$$

It can be readily realized looking at (4.43) that net growth corresponds to  $J_g > 1$  and net death to  $J_g < 1$ . Of course,  $J_g$  never vanishes, otherwise  $\mathbf{F}_T$  would be singular. Applying the polar decomposition theorem to the growth tensor  $\mathbf{G}$  we are sure that there exist a unique rotation  $\mathbf{R}_g$  and a unique symmetric tensor  $\mathbf{U}_g$  such that  $\mathbf{G} = \mathbf{R}_g \mathbf{U}_g$ . However, for the arbitrariness of the choice of the natural configuration with respect to rotations, we can certainly choose it so that  $\mathbf{R}_g = \mathbf{I}$  and  $\mathbf{G} = \mathbf{U}_g$ .

Differentiating (4.45) and then using (3.14) rewritten here for sake of clarity

$$\frac{d}{dt}(\phi_T J_T) = \Gamma_T J_T, \quad (4.46)$$

one has

$$\dot{J}_N = -\frac{\phi_N}{\phi_T^2} \dot{\phi}_T = -\frac{\phi_N}{\phi_T} \left( \frac{\Gamma_T}{\phi_T} - \frac{\dot{J}_T}{J_T} \right), \quad (4.47)$$

or

$$\frac{\dot{J}_T}{J_T} - \frac{\dot{J}_N}{J_N} = \frac{\Gamma_T}{\phi_T}. \quad (4.48)$$

Recalling the splitting (4.42), one finally has

$$\frac{\dot{J}_g}{J_g} = \frac{\Gamma_T}{\phi_T}, \quad (4.49)$$

or defining the rate of growth tensor

$$\mathbf{D}_g = \text{sym}(\dot{\mathbf{G}} \mathbf{G}^{-1}), \quad (4.50)$$

one has from standard tensor calculus that

$$\dot{J}_g = J_g \text{tr } \mathbf{D}_g, \quad (4.51)$$

and therefore

$$\text{tr } \mathbf{D}_g = \frac{\Gamma_T}{\phi_T}. \quad (4.52)$$

Equation (4.52) reveals then that the first principal invariant of  $\mathbf{D}_g$  is the right hand side of the Eulerian mass balance equation (3.1) and the rate of mass production can be easily identified from one of the constitutive parameters of the material.

In particular, for isotropic growth,  $\mathbf{G} = g \mathbf{I}$  where  $g$  is a scalar, (4.49) rewrites

$$\frac{3\dot{g}}{g} = \frac{\Gamma_T}{\phi_T} \quad (4.53)$$

which for known  $\Gamma_T$  completely determines  $\mathbf{G}$ .

In general, however, growth requires to give constitutively a suitable evolution equation for the growth tensor, which may depend on a variety of quantities, e.g.

$$\dot{\mathbf{G}} = \mathcal{L}_g(\mathbf{X}, t, \mathbf{S}, \mathbf{G}, \mathbf{c}), \quad (4.54)$$

where  $\mathbf{c}$  is the set of nutrients and growth factors involved in growth and  $\mathbf{S}$  is a suitable invariant measure of stress which might contain information on the direction of principal stresses. The involvement of the quantities above implies a strong coupling between the growth tensor and mechanical and chemical terms, so that, in general, one cannot look at growth in time as being separated from the overall mechanical response and the chemical background. This means that Eq.(4.54) has to be solved simultaneously with the other evolution equations.

Finally, we observe that one can replace the mass balance equation (4.46) with

$$\frac{d}{dt}(\phi_T J_N) = 0, \quad (4.55)$$

an equation not involving growth, which is instead given constitutively and is related to  $\Gamma_T$  through (4.54) or (4.53) for isotropic growth. Equation (4.55) resembles the usual Lagrangean version of conservation of mass in the absence of mass sources but is related to a fictitious deformation from the natural configuration which is never achieved by the body.

The other constitutive relation to be specified regards the stress tensor. In their paper Ambrosi and Mollica [4] assumed that at any time the mechanical response of the tumor from the natural configuration is hyper-elastic.

In particular, they used a Blatz-Ko constitutive relation [13], a classical non-linear elastic model, which can be seen as a generalization of the classical Mooney-Rivlin model for rubber. The Blatz-Ko material is the simplest hyper-elastic compressible material and has been successfully applied to model polymeric foams, a system that shows some analogies with the mechanical behavior of cell aggregates [84].

The Cauchy stress tensor takes then the form

$$\mathbf{T}_T = \frac{\mu}{J_N} [-(J_N)^{-q} \mathbf{I} + \mathbf{B}_N], \quad (4.56)$$

where  $\mathbf{B}_N =: \mathbf{F}_n \mathbf{F}_N^T$  is the left Cauchy-Green stretch tensor, and  $\mu$  and  $q$  are positive material constants. Further comments on other possible constitutive choices are contained in the following section.

Their growth model inside the tumor can then be summarized as

$$\left\{ \begin{array}{l} \phi_T J_N = \phi_N, \\ \nabla \cdot \mathbf{T}_T = \mathbf{0}, \\ \dot{g} = \frac{g}{3} \frac{\Gamma_T}{\phi_T}, \\ \nabla \cdot (D \nabla n) - \delta \phi_T n = 0, \end{array} \right. \quad (4.57)$$

where the stress tensor is given by (4.56) and

$$\Gamma_T = \gamma \frac{n - n_0}{N - n_0} e^{-(s/s_0)^2} \phi_T \quad (4.58)$$

where  $s$  is the trace of the first Piola-Kirchoff stress tensor  $\mathbf{P} = J_T \mathbf{T}_T \mathbf{F}_T^{-T}$ .

This very simple equation assumes that stress always inhibits growth while net growth occurs if a sufficient minimum quantity of nutrient is available, otherwise one has that the body resorbs mass.

The aim of the paper by Ambrosi and Mollica [3] was to compare the model with the experiments performed by Helmlinger et al. [50] who study the influence of external loading on tumor growth by letting a tumor spheroid grow in a gel.

In the experimental set-up agarose, a polysaccharide extracted from seaweed, is dissolved into boiling water. When the medium starts cooling down, the polysaccharide chains crosslink with each other, causing the solution to gel into a semi-solid matrix. The more agarose is dissolved in the boiling water, the firmer the gel is. While the solution is still fluid, the tumor cells are plugged into the polymerizing medium. After cooling, the tumor cells are trapped in the agarose gel that has known mechanical properties depending on the solid phase concentration. The nutrient rapidly diffuses in the liquid phase of the gel, thus providing a constant concentration at the boundary of the spheroid. As the spheroid grows, it displaces the surrounding gel, which in turn exerts a uniform compression on the tumor spheroid. By varying the volume fraction of the solid component during the preparation of the gel, they are able to modulate its stiffness and hence to apply different stress fields on the tumor.

The main result obtained in [50] is that the stress field definitely reduces the final dimensions of the spheroids. At a cellular level, though, spheroids cultured in gels of increasing stiffnesses are characterized by a decreased apoptosis rate with no significant change in proliferation rate and hence increased cellular packing. Moreover inner regions of free-suspension spheroids often exhibit large voids that were rarely seen in gel-cultured spheroids.

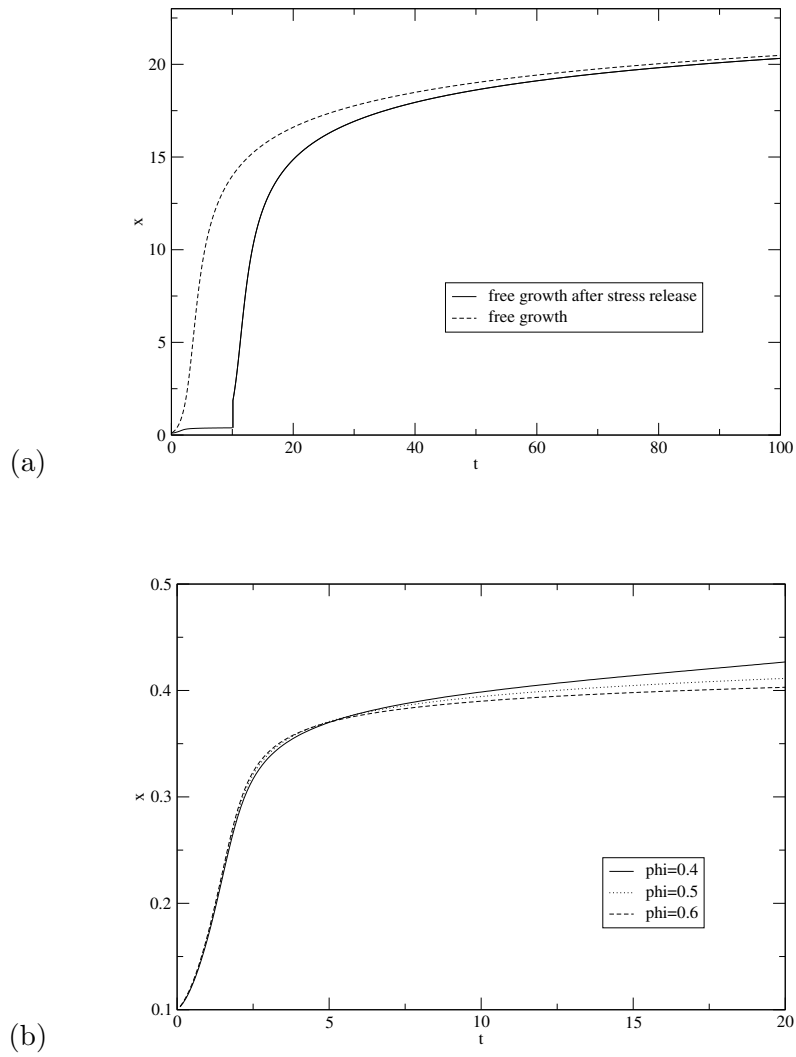


Figure 11: Comparison between free growth of a tumor spheroid (dashed line in (a)) and constrained growth ((b) and full line in (a)). At  $t = 10$  the spheroid is ideally extracted; being unloaded, it retains residual stress only. The plot of the subsequent increase in size shows that the past history tends to be asymptotically forgotten: the radius approaches the free one and residual stress vanishes. In (b) the evolution of the position of the interface between tumor and gel is given for different gel concentrations.

The agarose gel was modelled as a poroelastic material with constitutive equation given by

$$\mathbf{T} = \tilde{\gamma} \frac{\rho}{\rho_0} \frac{e^{\beta(I-3)}}{(\mathbb{I} - \phi_0^2)^\alpha} \left[ \beta \mathbf{B} - \alpha \frac{\mathbb{I}}{\mathbb{I} - \phi_0^2} \mathbf{I} \right], \quad (4.59)$$

where  $I$  and  $\mathbb{I}$  are the first and third invariants of the right Cauchy-Green deformation tensor  $\mathbf{C} = \mathbf{F}^T \mathbf{F}$  of the surrounding gel and  $\alpha = \beta(1 - \phi_0^2)$ .

The free boundary problem for the growth of an elastic tumor in a gel is completed by interfacing (4.57) and

$$\nabla \cdot \mathbf{T} = \mathbf{0}, \quad (4.60)$$

where  $\mathbf{T}$  is given in (4.59) with continuity of displacement and of the normal component of the stress thus providing the following interface conditions

$$\llbracket \mathbf{u} \cdot \mathbf{n} \rrbracket = 0, \quad (4.61)$$

$$\llbracket \mathbf{T} \mathbf{n} \rrbracket = \mathbf{0}, \quad (4.62)$$

where the jump is evaluated across the the interface and  $\mathbf{n}$  is its unit normal vector.

In agreement with the experiments Ambrosi and Mollica [3] assumed spherical symmetry. Normalizing space length with the outer radius of the gel the tumor spheroid is assumed to be initially located in  $R \in [0, \bar{R}]$ , while the gel fills the space  $R \in [\bar{R}, 1]$ , where  $\bar{R}$  is chosen sufficiently smaller than one so that the effect of the external constraints on the growth of the spheroid can be neglected.

Figure 11 shows the evolution of a freely growing tumor, i.e., not in the gel and then without external loads. After an initial exponential growth and a transition period growth becomes linear in time. In the absence of external loads the change in growth rate is essentially due to the reduced availability of nutrient that occurs when the diameter of the spheroid overcomes the diffusion length of the nutrient in the spheroid.

This effect is confirmed by the plots of concentration depicted in Fig. 12a at different times: at  $t = 20$  the nutrient has a non-negligible concentration just in a thin layer around the border (the proliferating rim) so that the growth is essentially on the surface. Note that the existence of a proliferating rim, as described in the experimental literature, here arises without any *ad hoc* introduction. In principle, residual stresses due to non-homogeneous growth could inhibit proliferation too. However, the stress field generated in free growth is small and does not affect the size of the spheroid: in this case the key mechanism is the decreasing amount of nutrient available that influences the growth function  $g$  through the relationship (4.58), yielding the behavior of Fig. 12b.

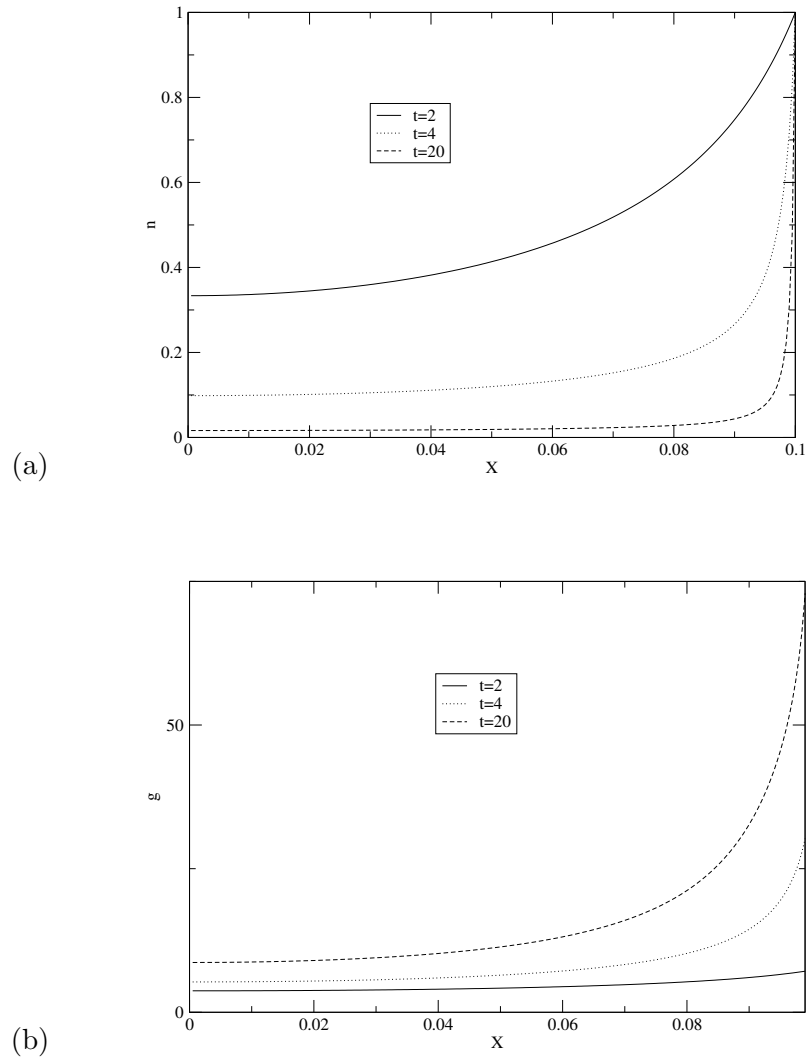


Figure 12: (a) Available nutrient concentration and (b) growth function in a freely growing tumor plotted versus undeformed radius at different times.

The position of the interface between a spheroid embedded in a poroelastic medium versus time is tracked in Fig. 11b for different concentrations of the solid component. The growth of the size of the spheroid is linear from the very beginning, until it becomes almost constant when the external stress starts inhibiting growth.

As the nutrient has a non constant spatial distribution in the tumor, the growth is not homogeneous and some residual stress is generated. The stress in the tumor is always compressive, the largest value occurring at the interface between spheroid and gel.

Looking carefully at the final size of the spheroid, one understands that the diameter is still much smaller than the freely floating one, while experimentally the final size of the embedded spheroid is some tenths of the freely growing one. This observation suggests that, despite growth inhibition by stress works fine as described in the present work, some mechanism of stress release must be included in the model in order to obtain a final size which is also in quantitative agreement with experiments.

After extracting from the gel a spheroid that was in its plateau-phase, cells restart duplicating, yielding the results shown in Fig. 11. When comparing the dashed line indicating the diameter of the spheroid growing after stress release with a free-growth one, one finds that the former tends just asymptotically to reach the latter so that, in some sense, the inhomogeneous original growth never completely vanishes. The slope discontinuity of the full line in Fig. 11a occurring at  $t = 10$  corresponds to gel extraction.

#### 4.4 Visco-Elasticity and Pseudo-Plasticity in Tumor Growth

The models presented in Sections 4.1–4.3 can be certainly improved by taking into account of the viscoelastic behavior that characterizes most biological materials. However, the characteristic times of the rate dependent response of the materials involved are of the order of tens of seconds and therefore much less than the characteristic times of cell duplication (a day), so in our opinion viscoelasticity only plays a secondary role in problems coupled with growth. Of course, it can have important effects in mechanical problems characterized by times of the order of the relaxation and retardation times, but in describing them growth can be in our opinion neglected, so that the two descriptions are somewhat complementary.

On the other hand, when treating the tumor as a solid there is an important effect that should not be neglected which has to do with the pseudo-plastic behavior of multicellular spheroids.

The cellular scale motivation of the macroscopic plastic behavior is the following. As shown in Fig. 2, cells adhere to each other via cadherin junctions and to the extra-cellular matrix via integrin junctions. These bonds have a limited strength as measured, for instance, by Baumgardner et al. [10] and Canetta et al. [21]. In fact, the adhesive strength of a single

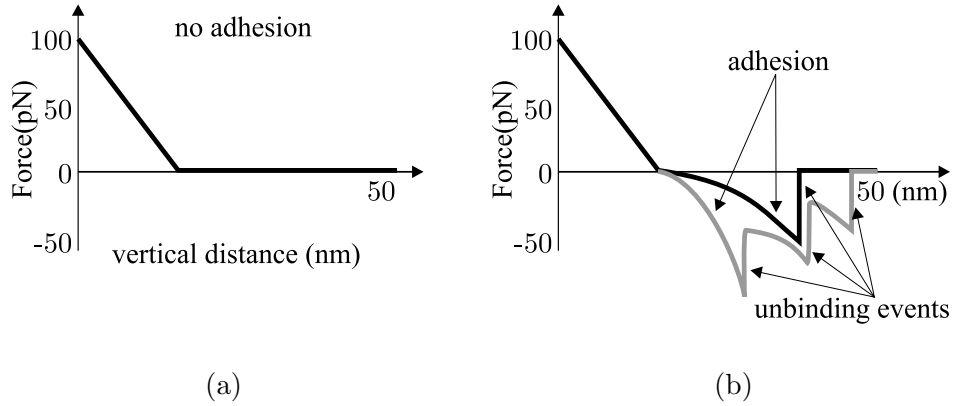


Figure 13: Adhesive force measurement. The positive branch refers to the compression of the cell by the bead. At larger distances the adhesive cell acts as an elastic nonlinear spring until single or multiple unbinding occurs (redrawn from [10]).

bond was found to be in the range of 35–55 pN. Since the density of VE-cadherin on a cell surface is about 400–800 molecules/ $\mu\text{m}^2$  of the surface one can estimate the resistance to pulling to be of the order of 0.1 kPa.

Typical experiments to test the adhesive strength of a cell consist in gluing a functionalized microsphere at the tip of an AFM cantilever (atomic force microscopy). After putting the microsphere in contact with the cell, the cantilever is pulled away at a constant speed (in the range 0.2–4  $\mu\text{m}/\text{sec}$ ). If there is no adhesion between the bid and the cell, the force measured has the behavior shown in Fig. 13a. This is experimentally obtained, for instance, by the addition of an antibody of the VE-cadherin external domain. On the other hand, adhesion gives rise to the measurement of a stretching force and a characteristic jump indicating the rupture of an adhesive bond, as shown in Fig. 13b. Actually, since a sphere binds to many receptors, it is common to experience multiple unbinding events occurring at different instants during the single experiment, as shown by the grey curve in in Fig. 13b.

Transferring this concept to tumor mechanics it is clear that if an ensemble of cells is subject to a sufficiently high tension or shear, then some bonds break and some others form, leading to the necessity to introduce plasticity in the description. This in particular occurs during growth when the duplicating cell need to displace its neighbors to make room for its sister cells as sketched in Fig. 15.

Generalizing the concepts introduced in the previous section, what is left when relieving the state of stress of a particle in the configuration  $\mathcal{K}_t$

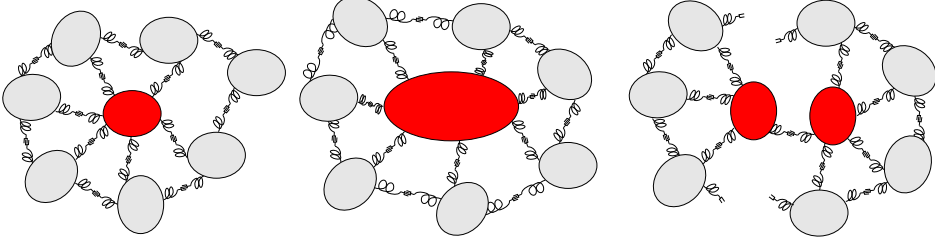


Figure 14: Sketch of pseudo-plastic behavior in tumor growth.

keeping its mass constant, includes both growth and plastic deformation due to unbinding events.

This means that focusing on the population of tumor cells, one need to generalise Fig. 8 to a three-step process which includes plastic deformations, i.e.

$$\mathbf{F}_T = \mathbf{F}_N \mathbf{F}_p \mathbf{G}_T . \quad (4.63)$$

From the biological point of view, it is not difficult to imagine the splitting, because as already stated the characteristic time of cell cycle is much longer than the times involved both in plastic and elastic phenomena.

Denoting by  $\mathcal{K}_p$  the intermediate configuration for the tumor between  $\mathcal{K}_0$  and  $\mathcal{K}_n$ , we will assume that for any given “particle” the volume ratio in  $\mathcal{K}_p$  is the same as in the natural configuration and in the original reference configuration, i.e.  $\phi_p = \phi_T(t = 0) = \phi_N$ .

The generalization of (4.43–4.45) gives

$$J_T = \frac{\phi_N}{\phi_T} \frac{dm}{dM} , \quad (4.64)$$

$$J_g = \frac{\phi_N}{\phi_p} \frac{dm}{dM} = \frac{dm}{dM} , \quad (4.65)$$

$$J_p = \frac{\phi_p}{\phi_N} = 1 , \quad (4.66)$$

$$J_N = \frac{\phi_N}{\phi_T} , \quad (4.67)$$

Notice that differentiating (4.67) one has

$$\frac{d}{dt} \log(\phi_T J_N) = 0 , \quad (4.68)$$

an equation similar to (4.55), where the time derivative is computed along any constituent.

In order to be more specific, we consider the tumor as a tri-phasic mixture made of ECM, extracellular liquid and cells, as in Section 4.1. However, contrary to Section 4.1, in this section we will neglect ECM remodelling. The extracellular matrix can then be viewed as a substrate on which cells move and duplicate and from the mechanical point of view its presence results very useful because it can represent a suitable framework to properly define a Lagrangean coordinate system. Equation (3.8) with  $\Gamma_0 = 0$  and  $\Gamma_\ell = -\Gamma_T$  can be written in the Lagrangean form just defined as

$$\frac{d_0}{dt}(\phi_0 J_0) = 0, \quad (4.69)$$

$$\frac{d_0}{dt}(\phi_T J_0) + \text{Div}_0[\phi_T J_0 \mathbf{F}_0^{-1}(\mathbf{v}_T - \mathbf{v}_0)] = \Gamma_T J_0, \quad (4.70)$$

$$\frac{d_0}{dt}(\phi_\ell J_0) + \text{Div}_0[\phi_\ell J_0 \mathbf{F}_0^{-1}(\mathbf{v}_\ell - \mathbf{v}_0)] = -\Gamma_T J_0, \quad (4.71)$$

where  $d_0/dt$  is the time derivative following the ECM,  $\text{Div}_0$  is the divergence operator with respect to the ECM and  $\mathbf{F}_0$  is the deformation gradient of the ECM.

Note that summing the mass balance equations, thanks to the saturation assumption and the fact that the mixture is closed one has

$$\frac{d_0 J_0}{dt} + \text{Div}_0[J_0 \mathbf{F}_0^{-1}(\mathbf{v}_c - \mathbf{v}_0)] = 0, \quad (4.72)$$

where  $\mathbf{v}_c = \phi_T \mathbf{v}_T + \phi_\ell \mathbf{v}_\ell + \phi_0 \mathbf{v}_0$ .

Following a procedure similar to that used to obtain Eqs. (4.48)-(4.52) one can write

$$\frac{1}{J_0} \frac{d_0 J_0}{dt} - \frac{1}{J_N} \frac{d_0 J_N}{dt} = \frac{\Gamma_T}{\phi_T} - \frac{1}{\phi_T J_0} \text{Div}_0[\phi_T J_0 \mathbf{F}_0^{-1}(\mathbf{v}_T - \mathbf{v}_0)], \quad (4.73)$$

while

$$\frac{1}{J_g} \frac{d_0 J_g}{dt} = -\frac{1}{J_p} \frac{d_0 J_p}{dt} - \frac{1}{J_0} \frac{d_0 J_0}{dt} + \frac{1}{J_T} \frac{d_0 J_T}{dt} \quad (4.74)$$

$$+ \frac{\Gamma_T}{\phi_T} - \frac{1}{\phi_T J_0} \text{Div}_0[\phi_T J_0 \mathbf{F}_0^{-1}(\mathbf{v}_T - \mathbf{v}_0)], \quad (4.75)$$

where the first term on the r.h.s. vanishes because of (4.66)-(4.52). This relation is not so good looking as (4.51) because we are using a Lagrangean framework based on a constituent different from the one that is duplicating.

Equation (4.75) can be re-written in a slightly more compact form as

$$\frac{d_0}{dt} \log \frac{J_g J_0}{J_T} = \frac{\Gamma_T}{\phi_T} - \frac{1}{\phi_T J_0} \text{Div}_0[\phi_T J_0 \mathbf{F}_0^{-1}(\mathbf{v}_T - \mathbf{v}_0)], \quad (4.76)$$

while, recalling (4.70), Eq.(4.73) can be simplified to

$$\frac{d_0}{dt} \log(\phi_T J_N) = 0, \quad (4.77)$$

an equation similar to (4.55).

If tumor cells are assumed to grow isotropically, so that  $\mathbf{G}_T = g_T \mathbf{I}$ , one then has that  $\mathbf{F}_N = g_T^{-1} \mathbf{F}_T \mathbf{F}_p^{-1}$  and

$$\frac{3}{g_T} \frac{d_0 g_T}{dt} = \frac{1}{J_0} \frac{d_0 J_0}{dt} + \frac{1}{J_T} \frac{d_0 J_T}{dt} + \frac{\Gamma_T}{\phi_T} - \frac{1}{\phi_T J_0} \text{Div}_0[\phi_T J_0 \mathbf{F}_0^{-1}(\mathbf{v}_T - \mathbf{v}_0)], \quad (4.78)$$

where  $\Gamma_T$  has to be given constitutively.

Coming to the momentum equation, following Section 3.1, the extracellular liquid is treated as an inviscid fluid in light of the usual assumptions used to get Darcy's law

$$\begin{cases} \mathbf{0} = -\phi_0 \nabla P + \nabla \cdot \hat{\mathbf{T}}_0 - \mathbf{M}_{T0}(\mathbf{v}_0 - \mathbf{v}_T), \\ \mathbf{0} = -\phi_T \nabla P + \nabla \cdot \hat{\mathbf{T}}_T + \mathbf{b}_T + \mathbf{M}_{\ell T}(\mathbf{v}_\ell - \mathbf{v}_T) - \mathbf{M}_{T0}(\mathbf{v}_T - \mathbf{v}_0), \\ \mathbf{0}_\ell = -\phi_\ell \nabla P - \mathbf{M}_{\ell T}(\mathbf{v}_\ell - \mathbf{v}_T). \end{cases} \quad (4.79)$$

As in Section 3.1, introducing  $\mathbf{K}$  and  $\mathbf{K}_0$  and writing the momentum equation of the mixture, one can write

$$\begin{cases} \mathbf{0} = -\phi_0 \nabla P + \nabla \cdot \hat{\mathbf{T}}_0 - \mathbf{K}_0^{-1}(\mathbf{v}_0 - \mathbf{v}_T), \\ \mathbf{v}_\ell - \mathbf{v}_T = -\mathbf{K} \nabla P, \\ \mathbf{0} = -\nabla P + \nabla \cdot (\hat{\mathbf{T}}_0 + \hat{\mathbf{T}}_T) + \mathbf{b}_T, \end{cases} \quad (4.80)$$

which can be written in the Lagrangean framework defined by the ECM.

Having in mind the need of including pseudo-plastic effects, we have to mention that while for the ECM one can take

$$\hat{\mathbf{T}}_0 = \mu_0 \phi_0 [-J_0^{-q_0} \mathbf{I} + \mathbf{B}_0], \quad (4.81)$$

to describe the behavior of the tumor cells we can distinguish two cases:

1. When and where the cell populations is subject to a moderate amount of stress, then the body behaves elastically, there are no plastic deformation, which means  $\mathbf{F}_p = \mathbf{I}$  and then  $\mathbf{F}_T = g_T \mathbf{F}_N$ .

2. When and where the stress overcomes a threshold Yield stress  $\sigma$  then the body behaves like a compressible liquid.

Referring to Figs. 13 and 14 one can argue that the resistance of a single bond is nearly constant, so that the threshold level distinguishing the appearance of plastic deformations is proportional to the amount of cells present in the sample. On this basis a constitutive equation of the following type can be suggested

$$\hat{\mathbf{T}}_T = \begin{cases} \mu\phi_T[-(J_N)^{-q}\mathbf{I} + \mathbf{B}_N], & \text{if } \sqrt{|\mathbb{I}_T|} < \phi_T\sigma; \\ \phi_T \left[ -\Sigma + \lambda_T(\nabla \cdot \mathbf{v}_T)\mathbf{I} + 2 \left( \eta + \frac{\sigma}{\sqrt{|\mathbb{I}_{2D}|}} \right) \mathbf{D} \right], & \text{if } \sqrt{|\mathbb{I}_T|} \geq \phi_T\sigma; \end{cases} \quad (4.82)$$

where  $\mathbb{I}_T$  is the second invariant of the stress tensor with the isotropic pressure omitted.

We notice that in one dimensional problems, the constitutive relation (4.82) re-writes

$$\hat{T}_{12} = \begin{cases} \mu\phi_T \frac{\partial u_x}{\partial Y}, & \text{if } \hat{T}_{12} < \phi_T\sigma; \\ \phi_T(\sigma + \eta\dot{\gamma}) & \text{if } \hat{T}_{12} \geq \phi_T\sigma; \end{cases} \quad (4.83)$$

where  $u_x$  is the displacement along the  $x$ -direction.

In order to describe possible shear-thinning effects,  $\eta$  can depend on  $\mathbb{I}_D$

$$\eta = m|\mathbb{I}_D|^{(n-1)/2} \quad (4.84)$$

where the coefficient  $n$  is related to the slope of the shear stress behavior versus the shear rate. In this way we obtain a constitutive equation similar to Herschel–Buckley model.

In order to be more realistic, one should take into account that ECM can be produced and cleaved, so that also for this constituent one should at least consider isotropic growth  $\mathbf{G}_0 = g_0\mathbf{I}$ . Luckily, as already mentioned in Section 2.2, the ECM is made of several constituents with different mechanical and chemical properties. Some of them continuously remodel, while others, like elastin, barely turnover [82]. This biological fact may be very useful to still define a proper and useful Lagrangean reference frame fixed on an ECM constituent, so that one can consider at the same time ECM remodeling, tumor growth and deformation of all constituents.

## 5 Future Perspective

It is becoming clearer and clearer that in addition to chemical signalling, mechanics plays an important role in tumor development not only to describe the mechanical interaction of the tumor with the surrounding tissues, but also for the interplay between mechanical properties of a tissue and the tumor developing in it. This opens up several new research directions which deserve further investigation.

Certainly, mathematical modelling still needs a characterization of the mechanical behavior of growing tissues, in order to quantify viscoelastic and plastic effect, to evaluate the importance of nonlinear effects and to identify the proper constitutive equation.

In this respect, for sake of completeness, it need be mentioned that in addition to the examples presented above several authors proposed linear elastic-type models with the inclusion of suitable growth contributions [7, 8, 9, 55], without splitting the deformation gradient into growth and deformation. More specifically, Jones and coworkers [55] propose

$$\mathbf{T}_T - \frac{1}{3}(\text{tr}\mathbf{T}_T)\mathbf{I} = \frac{2}{3}E \left( \mathbf{E}_T - \frac{1}{3}g_T\mathbf{I} \right), \quad (5.1)$$

where  $\mathbf{E}_T$  is the infinitesimal strain tensor and growth is assumed to be isotropic, or

$$\frac{D}{Dt}[\mathbf{T}_T - \frac{1}{3}(\text{tr}\mathbf{T}_T)\mathbf{I}] - \mathbf{W}_T\mathbf{T}_T + \mathbf{T}_T\mathbf{W}_T = \frac{2}{3}E \left( \mathbf{D}_T - \frac{1}{3}(\nabla \cdot \mathbf{v}_T)\mathbf{I} \right) \quad (5.2)$$

where  $D/Dt$  is the material time derivative following the tumor and  $\mathbf{W}_T$  is the spin tensor, while Araujo and McElwain [7, 8, 9] proposed

$$\frac{D}{Dt} \left[ \mathbf{T}_T - \frac{1}{3}(\text{tr}\mathbf{T}_T)\mathbf{I} \right] = 2\mu \left( \frac{D\mathbf{E}_T}{Dt} - (\nabla \cdot \mathbf{v}_T)\mathbf{G}_T \right) - \phi_T \frac{DP}{Dt}(3\mathbf{G}_T - \mathbf{I}) \quad (5.3)$$

where  $D/Dt$  is a convective derivative based on the tumor, and  $\mathbf{G}_T$  is a diagonal growth tensor.

The use of linear elasticity probably gives more freedom because it circumvents the difficulties implied by the definition of a proper Lagrangean framework. However, one has still to define what is a small deformation in a growing tumor. Probably, this is overcome by the introduction of plasticity and by the use of evolving natural configuration. In fact, as a first approximation then the deformation with respect to the configuration

achieved after the occurrence of plastic phenomena can be assumed to be small. Actually, one knows that for tensions larger than 0.1 kPa adhesion bonds break up. It would then be very interesting to correctly frame the linear elastic approach suggested by the Authors above using the concept of evolving natural configuration.

Other issues that need to be investigated further concern how a tumor remodels the surrounding environment and how, viceversa, the environment influences tumor growth. In order to do that the multiphase models presented in this chapter should be generalized to include more constituents belonging to both the immune system and the stroma. In particular, the presence of macrophages and their migration toward the hypoxic regions is very important for the related immune response, the formation of chronic inflammations and their angiogenic side effect. On the other hand, the possibility of developing therapies based on the use of engineered macrophages should be supported by suitable mathematical models.

In the stroma it might be important to include other types of cells like fibroblasts related with the production of extracellular matrix or to distinguish the different constituents of the extra-cellular matrix, because, as already mentioned in Section 4.4, some of them are subject to stronger turnover and remodeling than others. The balance between the different constituents and their percentage influence the overall mechanical characteristics of the tissue and the formation of the different environments tumor cells live in. As already stated the entire remodeling process is strongly affected by the stresses and strains the tissue is subject to.

Going to the inner characteristics of the cells, the tumor itself may contain several, functionally-different clones which differentiate in their genetic status, e.g., cells with normal and abnormal expression of the tumor suppressor gene, p53 and hormone sensitive and insensitive cells.

In this respect, one of the breakthroughs in modelling tumor growth consists in including what happens inside the cells and therefore in developing multiscale models which take into account of the cascades of events recalled in Fig. 3 possibly joined with those involving growth factors.

The need of working in a multiscale framework is an almost unconsciously standard procedure in biology and medicine. In fact, in order to understand and describe the behavior of any biological phenomena, researchers in Life Sciences tend to go to the smallest scale possible, because they know, for instance, that the behavior of a cell and the interactions that it has with the surrounding environment depend on the chemistry inside it and, after all, on the content of genetic information, on the particular genetic expression, on the activation of proper protein cascades and on their cross influence. Of course, in order to do that one needs to have estimates on the affinity constants. In absence of such measurements, one could initially start with a Boolean reasoning. However, things become complicated

when there are loops and intersections between different cascades triggered by different events.

For instance, in the models presented in this chapter the role played by nutrients and growth promoting and inhibitory factors is considered secondary but it is not. So, it is important to develop models which consider both mechanical and chemical cues and establish the relative importance at the protein cascade level.

Another interesting problem which has not been studied yet is the growth of tumors in mechanically heterogeneous environment, which includes network structures like blood vasculature, airways, and lymphatic system, the interaction with physical barriers like bones and cartilages, and the pressure on the surrounding tissues.

However, whenever developing all the generalizations above, one has to keep in mind the difficulties in obtaining specific measurements from the biologists. For instance, quantifying the dependence of the production rates of extracellular matrix and matrix degrading enzymes from the level of stress and/or strain is not easy and data are not available yet, though the effect was put in evidence many years ago and is applied in clinical practice. Mathematical modelling urgently needs to be based on biological measurements. On the other hand, we are however sure that experimental research can be stimulated by the development of mathematical models that on the basis of known experimental evidences and data showing the importance of mechanical aspects go one step beyond what is known in biology and medicine.

---

### *Acknowledgements*

Partially supported by the European Community, through the Marie Curie Research Training Network Project HPRN-CT-2004-503661: Modelling, Mathematical Methods and Computer Simulation of Tumor Growth and Therapy.

---

## 6 \*

### References

- [1] J.A. Adam and N. Bellomo, Eds. (1996). **A Survey of Models on tumor Immune Systems Dynamics**, (Birkhäuser, Boston).

- [2] D. Ambrosi and F. Guana (2005). Stress modulated growth, *Math. Mech. Solids*, in press.
- [3] D. Ambrosi and F. Mollica (2002). On the mechanics of a growing tumor, *Int. J. Engng. Sci.* **40**: 1297–1316.
- [4] D. Ambrosi and F. Mollica (2004). The role of stress in the growth of a multicell spheroid, *J. Math. Biol.* **48**: 477–499.
- [5] D. Ambrosi and L. Preziosi (2002). On the closure of mass balance models for tumor growth, *Math. Mod. Meth. Appl. Sci.* **12**: 737–754.
- [6] R.P. Araujo and D.L.S. McElwain (2004). A hystory of the study of solid tumor growth: The contribution of mathematical modelling, *Bull. Math. Biol.* **66**: 1039–1091.
- [7] R.P. Araujo and D.L.S. McElwain (2005). A mixture theory for the genesis of residual stresses in growing tissues, I: A general formulation, *SIAM J. Appl. Math.* **65**: 1261–1284.
- [8] R.P. Araujo and D.L.S. McElwain (2005). A mixture theory for the genesis of residual stresses in growing tissues, II: Solutions to the biphasic equations for a multicell spheroid, *SIAM J. Appl. Math.* **65**: 1285–1299.
- [9] R.P. Araujo and D.L.S. McElwain (2004). A linear-elastic model of anisotropic tumour growth, *Eur. J. Appl. Math.* **15**: 365–384.
- [10] W. Baumgartner, P. Hinterdorfer, W. Ness, A. Raab, D. Vestweber, H. Schindler, and D. Drenckhahn (2000). Cadherin interaction probed by atomic force microscopy, *Proc. Nat. Acad. Sci. USA* **97**: 4005–4010.
- [11] K.F. Becker, M.J. Atkinson, U. Reich, I. Becker, H. Nekarda, J.R. Siewert, and H. Hofler (1994). E-cadherin gene mutation provide clues to diffuse gastric carcinoma, *Cancer Res.* **54**: 3845–3852.
- [12] N. Bellomo and E. De Angelis, Eds. (2003). Special Issue on Modeling and simulation of tumor development, treatment, and control, *Math. Comp. Modeling* **37**.
- [13] P.J. Blatz and W.L. Ko (1962). Application of finite elasticity theory to the deformation of rubbery materials, *Trans. Soc. Rheology* **6**: 223–251.
- [14] C.J.W. Breward, H.M. Byrne, and C.E. Lewis (2002). The role of cell-cell interactions in a two-phase model for avascular tumor growth, *J. Math. Biol.* **45**: 125–152.

- [15] C.J.W. Breward, H.M. Byrne, and C.E. Lewis (2003). A multiphase model describing vascular tumor growth, *Bull. Math. Biol.* **65**: 609–640.
- [16] C.E. Brewster, P.H. Howarth, R. Djukanovic, J. Wilson, S.T. Holgate, and W.R. Roche (1990). Myofibroblasts and subepithelial fibrosis in bronchial asthma, *Am. J. Respir. Cell Mol. Biol.* **3**: 507–511.
- [17] L.F. Brown, A.J. Guidi, S.J. Schnitt, L. van de Water, M.L. Iruela-Arispe, T.-K. Yeo, K. Tognazzi, and H.F. Dvorak (1999). Vascular stroma formation in carcinoma in situ, invasive carcinoma and metastatic carcinoma of the breast, *Clin. Cancer Res.* **5**: 1041–1056.
- [18] F. Bussolino, M. Arese, E. Audero, E. Giraudo, S. Marchiò, S. Mitola, L. Primo, and G. Serini (2003). Biological aspects of tumour angiogenesis, in: **Cancer Modeling and Simulation**, L. Preziosi, Ed., Chapman & Hall/CRC Press, 1–22.
- [19] H.M. Byrne, J.R. King, D.L.S. McElwain, and L. Preziosi, (2003). A two-phase model of solid tumor growth, *Appl. Math. Letters* **16**: 567–573.
- [20] H.M. Byrne and L. Preziosi (2004). Modeling solid tumor growth using the theory of mixtures, *Math. Med. Biol.* **20**: 341–366.
- [21] E. Canetta, A. Leyrat, C. Verdier, and A. Duperray (2005). Measuring cell viscoelastic properties using a force-spectrometer: Influence of the protein-cytoplasm interactions, in press.
- [22] P. Carmeliet and R.K. Jain (2000). Angiogenesis in cancer and other diseases, *Nature*, **407**: 249–257.
- [23] M.A. Castilla, M.V.A. Arroyo, E. Aceituno, P. Aragoncillo, F. R. Gonzalez-Pacheco, E. Texeiro, R. Bragado, and C. Caramelo (1999). Disruption of cadherin-related junctions triggers autocrine expression of vascular endothelial growth factor in bovine aortic endothelial cells. Effect on cell proliferation and death resistance, *Circ. Res.* **85**: 1132–1138.
- [24] U. Cavallaro, B. Schaffhauser, and G. Christofori (2002). Cadherin and the tumor progression: Is it all in a switch?, *Cancer Lett.* **176**: 123–128.
- [25] L. Caveda, I. Martin-Padura, P. Navarro, F. Breviario, M. Corada, D. Gulino, M.G. Lampugnani, and E. Dejana (1996). Inhibition of cultured cell growth by vascular endothelial cadherin (cadherin-5/VE-cadherin), *J. Clin. Invest.* **98**: 886–893.

- [26] A.F. Chambers and L.M. Matrisian (1997). Changing views of the role of matrix metalloproteinases in metastasis, *J. Natl. Cancer Inst.* **89**: 1260–1270.
- [27] M.A.J. Chaplain, Ed. (1999). Special Issue *Math. Mod. Methods Appl. Sci.* **9**.
- [28] M.A.J. Chaplain, Ed. (2002). Special Issue on Mathematical Modeling and Simulations of Aspects of Cancer Growth, *J. Theor. Medicine* **4**.
- [29] M.A.J. Chaplain, (2006). **Mathematical Modelling of Tumour Growth**, Springer.
- [30] M. Chaplain, L. Graziano, and L. Preziosi (2005). Mathematical modelling of the loss of tissue compression responsiveness and its role in solid tumour development, *Math. Med. Biol.* In press.
- [31] M. Chiquet, M. Matthisson, M. Koch, M. Tannheimer, and R. Chiquet-Ehrismann (1996). Regulation of extracellular matrix synthesis by mechanical stress, *Biochem. Cell Biol.* **74**: 737–744.
- [32] G. Christofori and H. Semb (1999). The role of cell-adhesion molecule E-cadherin as a tumors-suppressor gene, *Trends Biochem. Sci.* **24**: 73–76.
- [33] S. Coats, W.M. Flanagan, J. Nourse, and J. Roberts (1996). Requirement of p27kip1 for restriction point control of the fibroblast cell cycle, *Science* **272**: 877–880.
- [34] P.S. Craft and A.L. Harris (1994). Clinical prognostic-significance of tumor angiogenesis, *Annals of Oncology*, **5**: 305-311.
- [35] E. Dejana, M.G. Lampugnani, M. Giorgi, M. Gaboli, and P.C. Marchisio (1990). Fibrinogen induces endothelial cell adhesion and spreading via the release of endogenous matrix proteins and the recruitment of more than one integrin receptor, *Blood* **75**: 1509–1517.
- [36] L. Deleu, F. Fuks, D. Spitkovsky, R. Hörlein, S. Faisst, and J. Rommelaere (1998). Opposite transcriptional effects of cyclic AMP-responsive elements in confluent or p27kip-overexpressing cells versus serum-starved or growing cells, *Molec. Cell. Biol.* **18**: 409–419.
- [37] C. Dietrich, K. Wallenfrang, F. Oesch, and R. Wieser (1997). Differences in the mechanisms of growth control in contact-inhibited and serum-deprived human fibroblasts, *Oncogene* **15**: 2743–2747.

- [38] M.J. Dorie, R.F. Kallman, D.F. Rapacchietta, D. Van Antwerp, and Y.R. Huang (1982). Migration and internalisation of cells and polystyrene microspheres in tumour cell spheroids, *Exp. Cell Res.* **141**: 201–209.
- [39] M.J. Dorie, R.F. Kallman, and M.A. Coyne (1986). Effect of Cytochalasin B Nocodazole on migration and internalisation of cells and microspheres in tumour cells, *Exp. Cell Res.* **166**: 370–378.
- [40] C.M. Elliot (1985). The Stefan problem with a non-monotone constitutive relation, *IMA J. Appl. Math.* **35**: 257–264.
- [41] D.R. Eyre (1979). Biochemistry of the intervertebral disk, *Int. Rev. Connect. Tissue Res.* **8**: 227–291.
- [42] J. Folkman (1974). Tumor angiogenesis, *Adv. Cancer Res.* **19**: 331–358.
- [43] J. Folkman and M. Hochberg (1973). Self-regulation of growth in three dimensions, *J. Exp. Med.* **138**: 745–753.
- [44] S.J. Franks, H.M. Byrne, J.R. King, J.C.E. Underwood, and C.E. Lewis (2003). Modelling the early growth of ductal carcinoma in situ of the breast, *J. Math. Biol.* **47**: 424–452.
- [45] S.J. Franks, H.M. Byrne, H.S. Mudhar, J.C.E. Underwood, and C.E. Lewis (2003). Mathematical modelling of comedo ductal carcinoma in situ of the breast, *Math. Med. Biol.* **20**: 277–308.
- [46] S.J. Franks and J.R. King (2003). Interactions between a uniformly proliferating tumor and its surrounding. Uniform material properties, *Math. Med. Biol.* **20**: 47–89.
- [47] J.P. Freyer and R.M. Sutherland (1986). Regulation of growth saturation and development of necrosis in EMT6/Ro multicellular spheroids by the glucose and oxygen supply, *Cancer Res.* **46**: 3504–3512.
- [48] C.J. Gottardi, E. Wong, and B.M. Gumbiner (2001). E-cadherin suppresses cellular transformation by inhibiting  $\beta$ -catenin signalling in an adhesion-independent manner, *J. Cell. Biol.* **153**: 1049–1060.
- [49] K.M. Harja and E.R. Fearon (2002). Cadherin and catenin alterations in human cancer, *Genes Chromosomes Cancer* **34**: 255–268.
- [50] G. Helmlinger, P.A. Netti, H.C. Lichtenbeld, R.J. Melder, and R.K. Jain (1997). Solid stress inhibits the growth of multicellular tumour spheroids, *Nature Biotech.* **15**: 778–783.

- [51] G. Helmlinger, P.A. Netti P.A., H.C. Lichtenbeld, R.J. Melder, and R.K. Jain (1997). Solid stress inhibits the growth of multicellular tumor spheroids, *Nature Biotech.* **15**: 778–783.
- [52] T. Hillen (2002). Hyperbolic models for chemosensitive movement, *Math. Mod. Meth. Appl. Sci.* **12**: 1007–1034.
- [53] T.L. Jackson and H.M. Byrne (2000). A mathematical model to study the effects of drug resistance and vasculature on the response of solid tumours to chemotherapy, *Math. Biosci.* **164**: 17–38.
- [54] P.R.A. Johnson (2001). Role of human airway smooth muscle in altered extracellular matrix production in asthma, *Clin. Exp. Pharm. Physiol.* **28**: 233–236.
- [55] A.F. Jones, H.M. Byrne, J.S. Gibson, and J.W. Dold (2000). A mathematical model of the stress induced during solid tumour growth, *J. Math. Biol.* **40**: 473–499.
- [56] A. Kato, H. Takahashi, Y. Takahashi, and H. Matsushime (1997). Inactivation of the cyclin D-dependent kinase in the rat fibroblast cell line, 3Y1, induced by contact inhibition, *J. Biol. Chem.* **272**: 8065–8070.
- [57] S.-G. Kim, T. Akaike, T. Sasagawa, Y. Atomi, and H. Kurosawa (2002). Gene expression of type I and type III collagen by mechanical stretch in anterior cruciate ligament cells, *Cell Struct. Funct.* **27**: 139–144.
- [58] M. Kjaer (2004). Role of extracellular matrix in adaptation of tendons and skeletal muscle to mechanical loading, *Physiol. Rev.* **84**: 649–698.
- [59] J. Klominek, K.H. Robert, and K.-G. Sundqvist (1993). Chemotaxis and haptotaxis of human malignant mesothelioma cells: Effects of fibronectin, laminin, type IV collagen, and an autocrine motility factor-like substance, *Cancer Res.* **53**: 4376–4382.
- [60] R. Kowalczyk (2005). Preventing blow-up in a chemotaxis model, *J. Math. Anal. Appl.* **305**: 566–588.
- [61] J.A. Lawrence and P.S. Steeg (1996). Mechanisms of tumor invasion and metastasis, *World J. Urol.* **14**: 124–130.
- [62] S. Levenberg, A. Yarden, Z. Kam, and B. Geiger (1999). p27 is involved in N-cadherin-mediated contact inhibition of cell growth and S-phase entry, *Oncogene* **18**: 869–876.

- [63] J.R. Levick (1987). Flow through interstitium and other fibrous matrices, *Q. J. Cogn. Med. Sci.* **72**: 409–438.
- [64] L.A. Liotta and E.C. Kohn (2001). The microenvironment of the tumor-host interface, *Nature* **411**: 375–379.
- [65] D. MacKenna, S.R. Summerour, and F.J. Villarreal (2000). Role of mechanical factors in modulating cardiac fibroblast function and extracellular matrix synthesis, *Cardiovasc. Res.* **46**: 257–263.
- [66] N. Mantzaris, S. Webb, and H.G. Othmer (2004). Mathematical modelling of tumour-induced angiogenesis, *J. Math. Biol.* **49**: 111–187 (2004).
- [67] J.J. Mao and H.-D. Nah (2004). Growth and development: Hereditary and mechanical modulations, *Amer. J. Orthod. Dentofac. Orthop.* **125**: 676–689.
- [68] L.M. Matrisian (1992). The matrix-degrading metalloproteinases, *Bioessays* **14**: 455–463.
- [69] D.M. Maurice (1984). The cornea and the sclera, in **The Eye**, H. Davson, Ed., Academic Press, 1–158.
- [70] V.C. Mow, M.H. Holmes, and W.M. Lai (1984). Fluid transport and mechanical problems of articular cartilage: A review, *J. Biomech.* **17**: 377–394.
- [71] Mow, V.C., and Lai, W.M., Mechanics of animal joints, *Ann. Rev. Fluid Mech.*, **11**, 247–288, (1979).
- [72] C.M. Nelson and C.S. Chen (2003). VE-cadherin simultaneously stimulates and inhibits cell proliferation by altering cytoskeletal structure and tension, *J. Cell Science* **116**: 3571–3581.
- [73] T. Oda, Y. Kanai, T. Okama, K. Yoshiura, Y. Shimoyama, W. Birchmeier, T. Sugimura, and S. Hirohashi (1994). E-cadherin gene mutation in human gastric carcinoma cell lines, *Proc. Natl. Acad. Sci. USA* **91**: 1858–1862.
- [74] K. Orford, C.C. Orford, S.W. Byers (1999). Exogenous expression of  $\beta$ -catenin regulates contact inhibition, anchorage-independent growth, anoikis, and radiation-induced cell cycle arrest, *J. Cell Biol.* **146**: 855–867.
- [75] K. Painter and T. Hillen (2002). Volume filling and quorum-sensing in models for chemosensitive movement, *Can. Appl. Math. Quart.* **10**: 501–543.

- [76] S.L. Parson, S.A. Watson, P.D. Brown, H.M. Collins, and R.J.C. Steele (1997). Matrix metalloproteinases, *Brit. J. Surg.* **84**: 160–166.
- [77] M.J. Paszek, N. Zahir, K.R. Johnson, J.N. Lakins, G.I. Rozenberg, A. Gefen, C.A. Reinhart-King, S.S. Margulies, M. Dembo, D. Boettiger, D.A. Hammer, and V. M. Weaver (2005) Tensional homeostasis and the malignant phenotype, *Cancer Cell* **8**: 241–254.
- [78] K. Polyak, J. Kato, M.J. Solomon, C.J. Sherr, J. Massague, J.M. Roberts, and A. Koff (1994). p27Kip1, a cyclin-Cdk inhibitor, links transforming growth factor- $\beta$  and contact inhibition to cell cycle arrest, *Genes & Develop.* **8**: 9–22.
- [79] L. Preziosi, Ed. (2003). **Cancer Modelling and Simulation**, CRC-Press/Chapman Hall.
- [80] L. Preziosi and A. Farina (2001). On Darcy’s law for growing porous media, *Int. J. Nonlinear Mech.*, **37**: 485–491.
- [81] P. Pujuguet, A. Hammann, M. Moutet, J. L. Samuel, F. Martin, and M. Martin (1996). Expression of fibronectin EDA+ and EDB+ isoforms by human and experimental colorectal cancer, *Am. J. Patho.* **148**: 579–592.
- [82] I.J. Rao, J.D. Humphrey, and K.R. Rajagopal (2003). Biological growth and remodeling: A uniaxial example with possible application to tendons and ligaments, *CMES* **4**: 439–455.
- [83] J.I. Risinger, A. Berchuck, M.F. Kohler, and J. Boyd (1994). Mutation of E-cadherin gene in human gynecological cancers, *Nature Genetics* **7**: 98–102.
- [84] T.W. Secomb and A.W. El-Kareh (2001). A theoretical model for the elastic properties of very soft tissues, *Biorheology* **38**: 305–317.
- [85] B. St. Croix, C. Sheehan, J.W. Rak, V.A. Florenes, J.M. Slingerland, and R.S. Kerbel (1998). E-cadherin-dependent growth suppression is mediated by the cyclin-dependent kinase inhibitor p27(Kip1), *J. Cell Biol.* **142**: 557–571.
- [86] W.G. Stetler-Stevenson, R. Hewitt, and M. Corcoran (1996). Matrix metallo–proteinases and tumor invasion: From correlation to causality to the clinic, *Cancer Biol.* **7**: 147–154.
- [87] A. Stockinger, A. Eger, J. Wolf, H. Beug, and R. Foisner (2001). E-cadherin regulates cell growth by modulating proliferation-dependent  $\beta$ -catenin transcriptional activity, *J. Cell. Biol.* **152**: 1185–1196.

- [88] R.M. Sutherland (1988). Cell and environment interactions in tumor microregions: the multicell spheroid model, *Science* **240**: 177-184.
- [89] T. Takeuchi, A. Misaki, S.-B. Liang, A. Tachibana, N. Hayashi, H. Sonobe, and Ohtsuki Y. (2000). Expression of T-cadherin (CDH13, H-cadherin) in human brain and its characteristics as a negative growth regulator of epidermal growth factor in neuroblastoma cells, *J. Neurochem.* **74**: 1489–1497.
- [90] J. Takeuchi, M. Sobue, E. Sato, M. Shamoto, and K. Miura (1976). Variation in glycosaminoglycan components of breast tumors, *Cancer Res.* **36**: 2133–2139.
- [91] S.C.G. Tseng, D. Smuckler, and R. Stern (1982). Comparison of collagen types in adult and fetal bovine corneas, *J. Biol. Chem.* **257**: 2627–2633.
- [92] Y. Tzukatani, K. Suzuki, and K. Takahashi (1997). Loss of density-dependent growth inhibition and dissociation of  $\alpha$ -catenin from E-cadherin, *J. Cell. Physiol.* **173**: 54–63.
- [93] S. Tzukita, M. Itoh, A. Nagafuchi, S. Yonemura, and S. Tsukita (1993). Submembrane junctional plaque proteins include potential tumor suppressor molecules, *J. Cell Biol.* **123**: 1049–1053.
- [94] E.B. Uglow, G.D. Angelini, and S.J. George (2000). Cadherin expression is altered during intimal thickening in humal saphenous vein, *J. Submicrosc. Cytol. Pathol.* **32**: C113–C119.
- [95] E.B. Uglow, S. Slater, G.B. Sala-Newby, C.M. Aguilera-Garcia, G.D. Angelini, A.C. Newby, and S.J. George (2003). Dismantling of cadherin-mediated cell-cell contacts modulates smooth muscle cell proliferation, *Circ. Res.* **92**: 1314–1321.
- [96] M.E. Warchol (2002). Cell proliferation and N-cadherin interactions regulate cell proliferation in the sensory epithelia of the inner ear, *J. Neurosci.* **22**: 2607–2616.
- [97] T.P. Witelski (1995). Shocks in nonlinear diffusion, *Appl. Math. Letters* **8**: 27–32.
- [98] S.L.-Y. Woo (1986). Biomechanics of tendon and ligaments, in **Frontiers in Biomechanics**, G.W. Schmid-Schonbein, S.L.-Y. Woo and B.W. Zweifach, Eds., Springer-Verlag, 180–195.
- [99] C.-M. Yang, C.-S. Chien, C.-C. Yao, L.-D. Hsiao, Y.-C. Huang, and C.B. Wu (2004). Mechanical strain induces collagenases-3 (MMP-13)

expression in MC3T3-E1 osteoblastic cells, *J. Biol. Chemistry* **279**: 22158–22165.

- [100] Y. Zhang, S. Nojima, H. Nakayama, J. Yulan, and H. Enza (2003). Characteristics of normal stromal components and their correlation with cancer occurrence in human prostate, *Oncol. Rep.* **10**: 207–211.